THE EVAPORATION OF HIGHLY CHARGED WATERDROPS IN THE ATMOSPHERE

by

YEAN MING HUANG

Department of Physics
Lakehead University
THUNDER BAY, ONTARIO, CANADA

Lakehead University

May, 1975

TABLE OF CONTENTS

Title	*Page*
Acknowledgement	*i*
Abstract	*ii*
List of Tables	*iii*
List of Figures	*iv*
1. INTRODUCTION	1
1-1 Historical Background	1
1-2 Aims of this Experiment	5
2. BASIC THEORY	7
2-1 Introduction	7
2-2 Rayleigh's Criterion	7
2-2-1 Introduction	7
2-2-2 Calculation of the Rayleigh's Criterion	7
2-3 Determination of the Radius and Charge of the Drop	20
3. APPARATUS	25
3-1 Main Description	25
3-2 Production of Fine Waterdrops by a Vibration Method	30
3-2-1 Introduction	30
3-2-2 Construction and Operation	31
3-2-3 Control of Droplets' Size and Frequency	35
3-2-4 Production of Highly Charged Droplets	35
3-2-5 Conclusion about the Vibration Method	36
3-3 Field and Time Control	36

Title *Page*

4. MEASUREMENTS 38

4-1 Procedure of Measurements 38

5. SOME DIFFICULTIES IN THE EXPERIMENT 40

5-1 The Drop 40
5-2 The Field 42
5-3 The Evaporation 42
5-4 Some Difficulties in the Measurement 45

6. RESULTS AND DISCUSSION 47

6-1 Results 47
6-2 The Uncertainties in the Experiment 65
6-3 The External Electric Field Affects the Results 66
6-4 The Evaporation Affects the Measurement 67

7. CONCLUSION 71

Appendix I Some Details of the Calculation of Rayleigh's Criterion 73
I-1 The Calculation of the Volume 73
I-2 Calculation of the Surface Area 74
I-3 Calculation of Charge Density and Potential 75
Appendix II An A.P.L. program for Calculating the Radius, Charge and Critical Value of the Drops 78
Appendix III Sample Calculations of Charge, Radius and Critical Value 79

REFERENCES 81

ACKNOWLEDGEMENT

I would like to express my sincere thanks to my supervisor, Dr. John Hart, for his continued guidance and encouragement during the course of this investigation, Dr. Donald Schnitzler for his invaluable suggestions and Mr. George Anderson who helped me in the construction of the apparatus for this experiment.

ABSTRACT

The evaporation of charged waterdrops is accompanied by negligible loss of charge; consequently, as the surface area falls, the electrostatic pressure increases. When a critical value is reached, one or more highly charged drops are ejected, the electrostatic pressure falls, and stability is regained.

Experimental work is carried out by levitating the charged drops in the electric field. The range of drop radii studied in this experiment is from 90 to 40 μm. The average radius loss was found to be about 8% per disintegration, with a charge loss of about 20%. According to Rayleigh's criterion, the drop will become unstable when the critical function,

$$\frac{k_1 Q^2}{4\pi(n+2)\gamma R^3},$$

rises to the critical value of 1. Here, k_1 is a constant, n is an integer greater than or equal to 2, R is the radius of the drop, Q is its charge and γ is the coefficient of surface tension for the liquid. Under normal conditions, the integer n in this critical function is 2. A higher value of n might represent a supercritical condition. In our experiment, the critical value was found always larger than 1, although previous experimental workers have agreed with the value 1. The critical value is higher than expected but there is internal consistency and the disintegration point is predictable: the disintegration always happens when the critical value reaches a specified, highest value.

The mass loss during the disintegration found by earlier workers is checked in this experiment and suggestions are made for more precise methods of measurement.

LIST OF TABLES

Table		*Page*
3-1	Major Components of Apparatus	28
6-1	Data for figure 6-1	53
6-2	Data for figure 6-2	54
6-3	Data for 9 Cases in Radius and Charge Loss	61
6-4	Data for figure 6-3a, 6-3b	63

LIST OF FIGURES

Figure		*Page*
1-1	A Charged Spherical Drop	2
1-2	A Charged Drop Levitated in the Atmosphere by the Electric Field	2
2-1	Coordinates Used to Describe the Surface of the Drop	9
2-2	Definition of the Angle ν	11
2-3	Motionless Charged Drop Levitated by the Electric Field	21
2-4	Charged Drop Falling Under Reduced Electric Field	21
3-1	General View of Experimental Apparatus	26
3-2	Gate Device of the Hole on the Top Electrode	27
3-3	Vibrating Needle for Producing Charged Drops	32
3-4	Constructional Details of the Vibrating Needle Device	33
3-5	Diagram of Circuit for Reducing the Electric Field	37
5-1	Uncharged Drops are Thrown about 7 cm Away From the Centre Hole	41
5-2	Charged Drops are Thrown even Farther	41
5-3	Ideally, the Drops can get into the Electric Field Vertically	41
5-4	The Drops are Repelled by the Glass Wall and Enter the Electrode	41
5-5a	The Shape of the Electric Field Without Grounding Foil	43
5-5b	The Shape of the Electric Field with Grounding Foil	43
6-1	Radius, Charge and Critical Value Plotted Against Time for a Typical Negatively Charged Drop	48

Figure *Page*

6-1a Graph of Radius vs Time 49
6-1b Graph of Charge vs Time 50
6-1c Graph of Critical Value vs Time 51
6-2 Radius, Charge and Critical Value Plotted Against Time for a Typical Positively Charged Drop 52
6-2a Graph of Radius vs Time 56
6-2b Graph of Charge vs Time 57
6-2c Graph of Critical Value vs Time 58
6-3a The Radius vs Charge at Disintegration Point 59
6-3b The Radius vs Charge at Disintegration Point (After Correction) 60

1. INTRODUCTION

1-1 Historical Background

The stability of waterdrops in an electric field was first investigated a very long time ago. The interest arose because the mechanism is of basic importance in the production of lightning in thunderstorms (Taylor, 1964).

In 1882, Rayleigh published his famous paper, *On the Equilibrium of Liquid Conducting Masses Charged with Electricity*. He derived a criterion which in brief may be expressed as:

$$k_1 Q^2 < 4(n + 2)\pi R^3 \gamma \qquad (1\text{-}1)$$

for spherical drops of radius R, charge Q, and surface tension γ. The quantity n is an integer larger than or equal to 2 and k_1 is a constant, expressed in rationalized SI units (figure 1-1).

For values of charge greater than those satisfying the inequality 1-1, the criterion predicts that spherical drops should become unstable. Rayleigh worked from the basis that the potential will be changed by slightly deforming the drop and he also expressed a generalized potential energy as a function of Q, γ, and R. Details will be shown in section 2. Since then, many scientists have tried to investigate this phenomenon in the laboratory.

One way to do this is to allow charged drops to evaporate. Highly charged drops are levitated by an electric field in the atmosphere (figure 1-2): as the time goes on, each drop will decrease in size, but the charge will decrease at a slow rate with the result that the ratio of charge energy to surface energy will become too high for stability, and charge loss, disruption or both must occur.

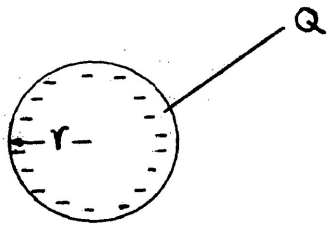

Fig. 1-1 A charged spherical drop

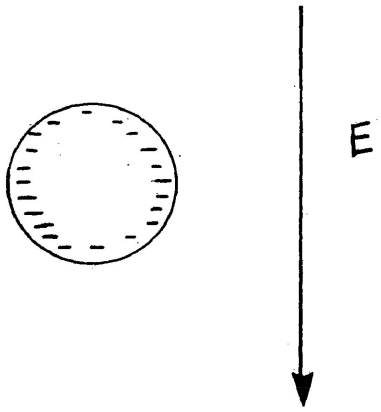

Fig. 1-2 A charged drop levitated in the atmosphere by the electric field.

A. Doyle, D. R. Moffett and B. Vonnegut (1964) first investigated this phenomenon by letting highly charged waterdrops spray into a chamber between two large electrodes where they levitated in an electric field. One drop was selected for observation. They found that after a period of time, say, several minutes, each charged drop suddenly fell down as if it had become very heavy. By abruptly increasing the electric field, the force balance would be reestablished before the drop hit the bottom electrode. During the evaporation, they found that the electric charge density on the surface of the drop increased to a value that produced a potential gradient of several hundreds of kilovolt per cm, until finally one or more small highly charged drops was ejected, the suspended drop thereby losing about 30% of its charge. After a complete observation, they let the drop fall on to a filter paper to measure its radius. Their results suggested that Rayleigh's criterion is correct.

Three years later, M. A. Abbas and J. Latham (1967) published their paper, considered as an extension of Doyle's work. The principle was almost the same, but the technique improved. They used a vibrational method to produce fine waterdrops. This method had the advantage of reducing the disturbance of the still air between the electrodes caused by the spray method. After they levitated the drops between the electrodes, they measured the radius and charge on the drops by timing the rate of fall of the drops. Thus was provided a continuous measurement of the drop before and after disintegration. The drop disintegrated to eject about 25% of its mass in the form of highly charged waterdrops and then stabilized. Their result was very close to Rayleigh's criterion.

But, this work was criticized by G. A. Dawson (1970) who pointed out that the external electric field intensity, although several orders of magnitude smaller than the radial field of the charged drops, can cause appreciable deviations from sphericity near the instability point even though the limiting value of charge is affected very little. (The external field intensity is usually between 5 and 20 volts per cm, and the radial field of the charged drops is usually several hundred kilovolts per cm. Details will be discussed in section 6.) He also pointed out that this kind of experiment might be not good for verifying the theoretically predicted behaviour of an isolated drop, although it probably does model quite well the behaviour of droplets evaporating in the electric field of the atmosphere. The levitating field in the laboratory experiment is very close to the actual electric field in the atmosphere. Later, in 1972, P. R. Brazier-Smith pointed out that with charged drops one could not use the spherical assumption although it was applied with considerable success to study the stability of uncharged drops.

Despite (or perhaps because of) these two reasons, research in this experiment was still believed to be worthwhile. In 1973, G. A. Dawson published his paper, *Charge Loss Mechanism of Highly Charged Waterdroplets in the Atmosphere*. In this paper, he studied at reduced pressure, the loss of charge mechanism and concluded that, at sea level, instability will be the dominant loss process; at higher altitudes, the charge loss for drops will probably be by ion collection. The size of the droplets and the electric field in the atmosphere determine which of these charge loss mechanisms will dominate. He pointed out that basically Rayleigh's criterion still held. The main

difference between his results and those of Abbas and Latham was the mass loss during the disintegration. Dawson found the mass loss to be just a few percent, but Abbas and Latham found it to be 25%.

This is the main interest in this thesis. The big difference in mass loss could be caused by a high and variable evaporation rate resulting from poor control of humidity and temperature. It is worthwhile to investigate in more detail the charge loss mechanism by ion collection.

1-2 Aims of this Experiment

The evaporation of highly charged waterdrops is an interesting experiment. This is true not only because it can apply to the production of lightning in thunderstorms, but also because it provides a good opportunity to look into the basic relation between temperature, humidity, pressure and charge. The main interest in this thesis is to investigate the different mass losses found by earlier workers and the possible effect of the ambient temperature and humidity.

Rayleigh's criterion expressed in a mathematical analysis follows the work done by C. D. Hendricks and J. M. Schneider (1963).

Different ways to set up the experiment have been tried. For producing fine drops, atomizers and hypodermic needles both have their disadvantages: an atomizer disturbs the still air inside the field; the hypodermic needle needs a high pressure to press the liquid. Some new apparatus is added to the arrangement of Abbas and Latham. The humidity is increased by evaporating water into the system, the temperature is continuously monitored and a TV videocorder is set up for recording the data.

Some difficulties of the experiment are the difficulty of producing drops, the nonuniformity of the field, the evaporation rate of the drops and the general low level of accuracy of the measurement.

The results are expressed in graphs of radius, charge and critical value *vs* time. The results of the experiment are quite reproducible. The average mass loss of the drop is about 23% per disintegration and charge loss is about 20%. Although the critical value in this experiment is higher than the results of earlier workers, it still predicts the disintegration quite well.

2. BASIC THEORY

2-1 Introduction

The forces acting on a charged waterdrop in an electric field include the surface tension and electrostatic force. In this section we calculate the forces on the drop, including the effect of the shape of the drop. Rayleigh's criterion was derived from the calculation of this force. Most of these calculations follow the work done by C. D. Hendricks and J. M. Schneider (1963). Further details of the calculation are given in Appendix I.

The theory of measuring the radius and charge is presented in section 2-2. An A.P.L. program used for the calculations is shown in Appendix II.

2-2 Rayleigh's Criterion

2-2-1 Introduction

In 1882, Rayleigh published his famous paper, *On the Equilibrium of Liquid Conducting Masses Charged with Electricity*, pointing out that charged liquid drops could become unstable under many circumstances, depending on the charges carried, surface tension, drop's size and so on. The results were widely used and quoted but, like much of Rayleigh's work, old notation and omitted steps make the derivation of these results difficult to understand. In 1963, C. D. Hendricks and J. M. Schneider successfully obtained the criterion in a somewhat more modern and comprehensible fashion. In this thesis, I use Hendricks' and Schneider's work as a basis to develop a detailed calculation of Rayleigh's criterion.

2-2-2 Calculation of Rayleigh's Criterion (after Hendricks and Schneider)

In the beginning of this calculation we state a fundamental theorem from classical mechanics. This will be used in what follows: it is that for any system engaged in vibrations of sufficiently small amplitude

about a position of stable equilibrium, the excursions from equilibrium are simple harmonic oscillations. For small displacements the potential energy function will be a homogeneous quadratic function of generalized coordinates. What we seek in this calculation is a potential energy function that is a homogeneous quadratic function of the generalized coordinates.

First, let us assume a charged drop that is cylindrically symmetric and, in shape, differs little from a sphere. The equation of this spheroid can be written in the following form:

$$r = a_o + \sum_{n=1} a_n P_n (\cos \theta) \qquad (2\text{-}1)$$

where r is the distance from the origin to the surface of spheroid, $a_n << a_o$ for all n, P_n is the Legendre Polynomial of order n, and θ is the angle between the z-axis and radial direction. (See fig. 2-1.) a_o and a_n are assume to be functions of time only.

The volume of spheroid of equilibrium is calculated as follows:

$$dV = r^2 \sin \theta \, d\phi d\theta dr$$

$$V = \int_o^r \int_o^\pi \int_o^{2\pi} r^2 \sin \theta \, d\phi d\theta dr$$

$$= \frac{2}{3} \pi \int_{-1}^{1} r^3 d\mu. \qquad (2\text{-}2)$$

Here, we let $\mu = \cos \theta$. Using the binomial theorem in the form:

$$(1 + x)^\alpha = 1 + \alpha x + [\alpha(\alpha - 1)/2!]x^2 + - - -$$

if $x << 1$ (2-3)

to expand r, and substituting in equation (2-2), we obtain the following expression for the volume of the spheroid:

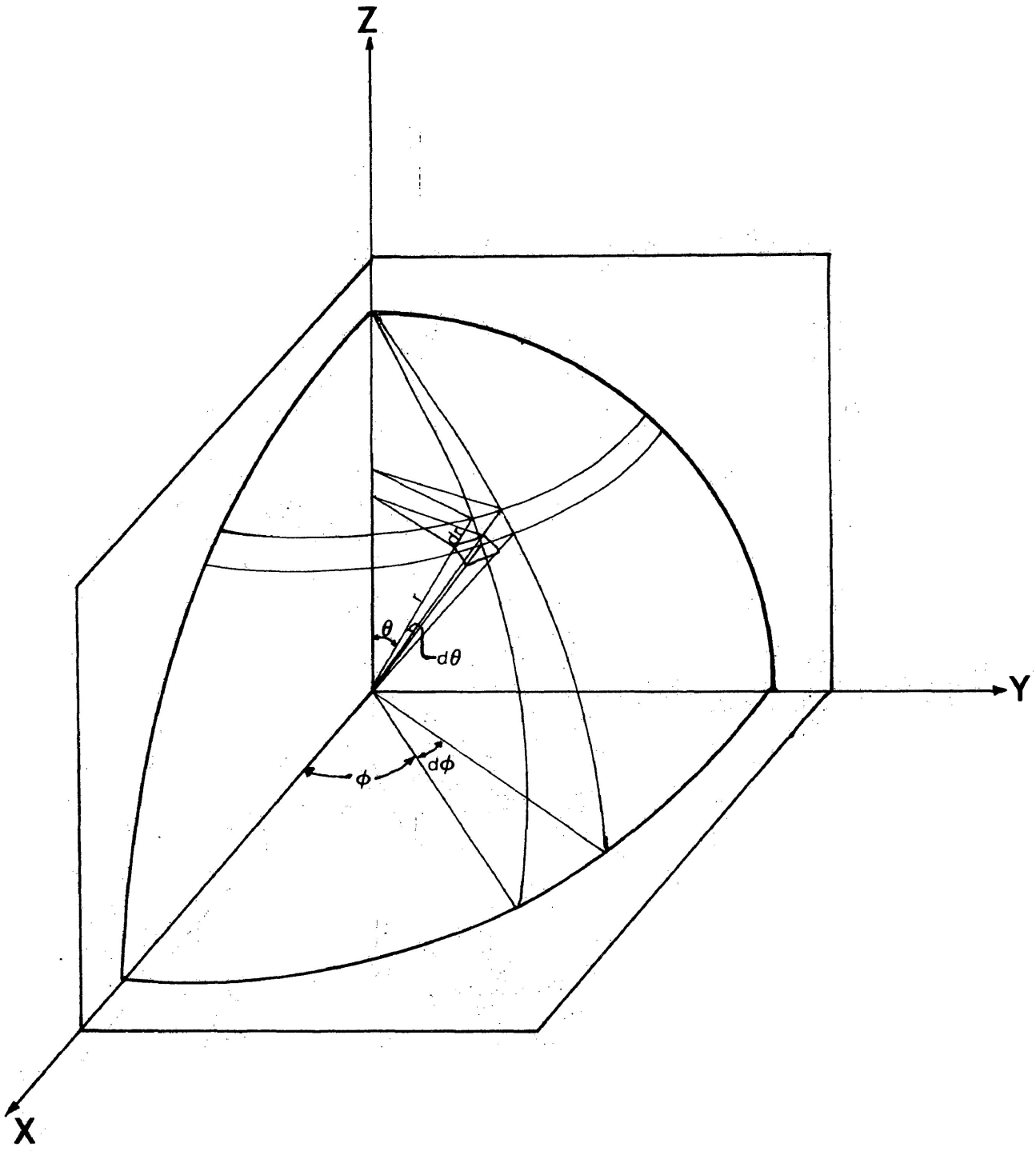

Fig. 2-1 Coordinates used to describe the surface of the drop

$$V = \frac{2}{3}\pi \int_{-1}^{1} a_o^3 \left[1 + 3\sum_n \frac{a_n}{a_o} P_n(\mu) + 3\sum_{nm}\sum \frac{a_m a_n}{a_o^2} P_n(\mu)P_m(\mu)\right]d\mu.$$

The first term of integration I_1 will become $\frac{4}{3}\pi a_o^3$, the second term I_2 will become 0, the third term will become $2\pi a_o^3 \sum_n \frac{2}{2n+1}\frac{a_n^2}{a_o^2}$.

Details of the calculations are given in Appendix I-1.

Summarizing the result, we get volume V equal to:

$$V = \frac{4}{3}\pi a^3, \text{ where } a = a_o\left(1 + \sum_n \frac{1}{2n+1}\left(\frac{a_n}{a_o}\right)^2\right) \text{ is the raduis.} \qquad (2\text{-}4)$$

This radius is that of a sphere of equal volume to that of the spheroid.

The potential energy due to the surface tension is equal to the surface tension multiplied by the increase in surface area of spheroid over the arbitrary reference surface. The arbitrary reference surface is taken as the sphere of equilibrium.

The area is given by

$$S = \int_0^{2\pi}\int_0^{\pi} \frac{r^2 \sin\theta}{\cos\nu}\, d\theta d\phi \qquad (2\text{-}5)$$

where θ and ϕ are usual spherical coordinate variables, and ν is the angle between normal to the surface and a radial line from the origin through the surface point in question. (See fig. 2-2.) If the equation of the surface is $F(r,\theta,\phi) = 0$, the normal vector is given by ∇F.

$$F(r,\theta,\phi) = r - a_o - \sum_{n=1} a_n P_n(\cos\theta) = 0 . \qquad (2\text{-}6)$$

Suppose $\vec{U}_r$, $\vec{U}_\theta$, $\vec{U}_\phi$ are the unit vector of r, θ, ϕ direction.

$$\nabla F(r,\theta,\phi) = \frac{\partial F}{\partial r}\vec{U}_r + \frac{1}{r}\frac{\partial F}{\partial \theta}\vec{U}_\theta + \frac{1}{\gamma \sin\theta}\frac{\partial F}{\partial \phi}\vec{U}_\phi$$

$$= \vec{U}_r + \sum_{n=1} \frac{a_n}{r}\sin\theta \frac{d}{d\mu}P_n(\mu)\vec{U}_\theta \qquad (2\text{-}7)$$

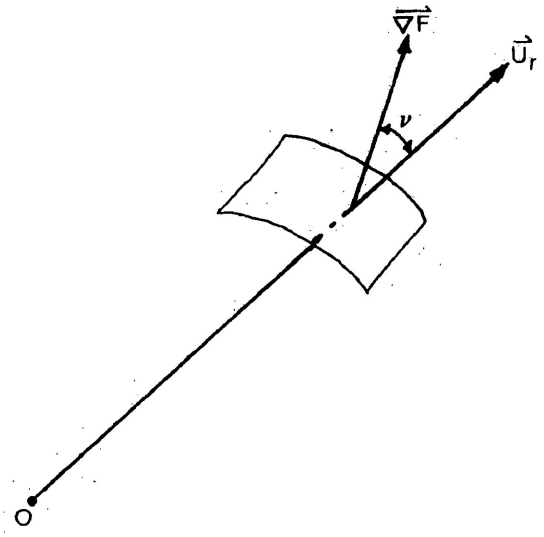

Fig. 2-2 Definition of the angle ν

where $\mu = \cos\theta$ again.

Thus, the absolute value $|\nabla F|$ is:

$$|\nabla F| = \left[1 + \left(\sum_{n=1} \frac{a_n}{r} \sin\theta \frac{d}{d\mu} P_n(\mu)\right)^2\right]^{\frac{1}{2}} . \qquad (2\text{-}8)$$

The quantity $\cos\nu$ is given by:

$$\cos\nu = \frac{\nabla F \cdot \vec{U}_r}{|\nabla F|} .$$

Using (2-7) and (2-8), we find

$$\cos\nu = \left[1 + \left(\sum_{n=1} \frac{a_n}{r} \frac{dP_n(\mu)}{d\mu} \sin\theta\right)^2\right]^{-\frac{1}{2}} \qquad (2\text{-}9)$$

$$(\cos\nu)^{-1} \approx \left[1 + \frac{1}{2}\sum_{m,n} \frac{a_n a_m}{r^2} \frac{dP_n(\mu)}{d\mu} \frac{dP_m(\mu)}{d\mu} (1 - \mu^2)\right]. \qquad (2\text{-}10)$$

Substituting (2-10) back onto (2-5), we get:

$$S = \int_0^{2\pi} \int_{-1}^{1} r^2 d\mu d\phi + \frac{1}{2} \int_0^{2\pi} \int_{-1}^{1} \sum_{m,n} a_n a_m \frac{dP_n(\mu)}{d\mu} \frac{dP_m(\mu)}{d\mu} (1 - \mu^2) d\mu$$

$$= 4\pi a_o^2 + 4\pi \sum_{n=1} (2n + 1)^{-1} a_n^2 + 2\pi \sum_{n=1} n(n+1)(2n + 1)^{-1} a_n^2 .$$

Details are shown in Appendix I-2.

This equation can be rewritten as:

$$S = 4\pi\left[a_o^2 + 2\sum_{n=1} (2n + 1)^{-1} a_n^2\right] - 4\pi \sum_{n=1} (2n + 1)^{-1} a_n^2$$

$$+ 2\pi \sum_{n=1} n(n + 1)(2n + 1)^{-1} a_n^2 . \qquad (2\text{-}11)$$

The first bracket can be recognized from (2-3) and (2-4) as a^2. Hence

$$S = 4\pi a^2 + 2\pi \sum_{n=1} (n - 1)(n + 2)(2n + 1)^{-1} a_n^2 \qquad (2\text{-}12)$$

where the last two terms of (2-11), have been combined to give the last term in (2-12). If γ is the surface tension, the potential energy of capillarity calculated from the sphere of equilibrium is:

$$P.E. = 2\pi\gamma \sum_{n} (n - 1)(n + 2)(2n + 1)^{-1} a_n^2 \ . \qquad (2\text{-}13)$$

There is another potential energy present with charged droplets, the static electric potential energy. If we can also express this stored energy approximately as a homogeneous quadratic function of the a_n, we will be able to consider the a_n as generalized coordinates for the spheroid. We seek an approximation that leads to this result. A suitable approximation is to calculate the charge density correct to the first order, then use this charge density to calculate the second-order perturbation in potential energy.

The equation of the spheroid is then written as:

$$r = a_o + \sum_n a_n P_n(\mu) \approx a + \sum_n a_n P_n(\mu), \qquad (2\text{-}14)$$

since a is different from a_o by a second-order quantity and we just want to calculate the charge density correct to the first order.

The electrostatic potential outside the conducting spheroid may be expanded in the harmonic series:

$$\Phi = k_1 \sum_{n=0} B_n \, r^{-n-1} \, P_n(\mu)$$

where the constants B_n are such that

$n \geq 1$, $B_n << B_o$ since $a_n << a_o$. Rationalized SI units are used, so $k_1 = \frac{1}{4\pi\varepsilon_o} = 9 \times 10^9 \frac{Nm^2}{C^2}$. Here, we recognize from the theory of multiples that $B_o = Q$, the total charge on the drop. Since $P_o(\mu) = 1$, we can rewrite the series as

$$\Phi = k_1\left(\frac{Q}{r} + \sum_{n=1} B_n P_n(\mu) r^{-n-1}\right) \quad . \tag{2-15}$$

At the surface of the conductor the potential is a constant, namely Φ_o, where:

$$\phi_o = k_1\left(Q[a + \sum_n a_n P_n(\mu)]^{-1} + \sum_{n=1} B_n P_n(\mu)[a + \sum_n a_n P_n]^{-n-1}\right).$$

Using the binomial theorem we find:

$$\Phi_o = k_1 Q[a^{-1}(1 - \sum_n \frac{a_n}{a} P_n(\mu))] + k_1 \sum_{n=1} B_n P_n(\mu)[a^{-n-1}\ (1 - \sum_n (n+1)\frac{a_n}{a} P_n(\mu))]$$

$$= \frac{Qk_1}{a} - \frac{Qk_1}{a}\sum_n \frac{a_n}{a} p_n(\mu) + k_1 \sum_{n=1} B_n P_n(\mu)\ [-\frac{1 - \sum_n (n+1)\frac{a_n}{a} P_n(\mu)}{a^{n+1}}] \ .$$

Because a_n and B_n are very small quantities, we may neglect the product of a_n and B_n, and we get

$$\Phi_o = \frac{k_1 Q}{a} - \frac{k_1 Q}{a}\sum_n \frac{a_n}{a} P_n(\mu) + \sum_n \frac{k_1 B_n P_n(\mu)}{a^{n+1}} \ . \tag{2-16}$$

Equating harmonics of the same order on both sides, we get:

$$\Phi = \frac{k_1 Q}{a} \quad , \quad Q a_n a^{n+1} = B_n a^2 \quad . \tag{2-17}$$

Substituting the relation of (2-17) back into (2-15), we find the potential of the spheroid is:

$$\phi = \frac{k_1 Q}{r} + \sum_{n=1} \frac{k_1 Q a_n a^{n-1}}{r^{n+1}} P_n(\mu) \ . \qquad (2\text{-}18)$$

The charge density on the surface of the spheroid is given by:

$$4\pi\sigma = -\nabla\phi \cdot \vec{n} \approx \frac{\partial \phi}{\partial r} \cos \nu \qquad (2\text{-}19)$$

where σ is the charge density, $\vec{n}$ is the unit vector normal to the surface, and ν is the angle between the normal to the surface and the radial direction. Since cos ν differs from 1 by just a small quantity, we may set cos ν equal to 1. Thus,

$$4\pi\sigma = -\frac{\partial \phi}{\partial r}\Big|_{r=a} + \sum_n a_n P_n(\mu)$$

$$= \frac{k_1 Q}{a^2} + Q k_1 \sum_{n=1} \frac{(n-1) a_n}{a^3} P_n(\mu). \qquad (2\text{-}20)$$

Detailed calculation is shown in Appendix I-3.

We may calculate, approximately, the second order change in potential by using this first order change in the charge density. Using the equation $\phi = \int \frac{\sigma}{r} dA$, we get:

$$\phi = \int_0^{2\pi} \int_{-1}^{1} \frac{\sigma r^2}{r} \, d\mu \, d\phi$$

$$= 2\pi k_1 \int_{-1}^{1} \frac{Q}{4\pi a^2} \left[1 + \sum_n (n-1) \frac{a_n P_n}{a}\right] \left[1 - \sum_n \frac{a_n P_n}{a}\right] a \, d\mu$$

$$= \frac{Qk_1}{a} - \frac{Qk_1}{a} \sum_n \frac{n-1}{2n+1} \frac{a_n^2}{a^2} \quad . \tag{2-21}$$

Detailed calculation is shown on the Appendix I-3.

The corresponding electrostatic potential energy, relative to the sphere of equilibrium, is

$$W = \frac{1}{2} Q\Phi$$

$$W = -\frac{k_1 Q^2}{2} \sum_n \frac{n-1}{2n+1} \frac{a_n^2}{a^3} \quad . \tag{2-22}$$

This is the homogeneous quadratic function of the a_n's that we were seeking. The minus sign here means the electrostatic force is opposed to the surface tension.

Now, we can calculate the kinetic energy for the drop. After the kinetic energy is found, we can form the Lagrangian function and find the time variation of a_n.

Since the drop is assumed homogeneous, inviscid and incompressible, we may assume the existence of a harmonic velocity potential Ψ. This velocity potential may be expanded in the series:

$$\Psi = \beta_o + \sum_{n=1} \beta_n r^n P_n(\mu) \quad . \tag{2-23}$$

The kinetic energy K is given:

$$K = \frac{1}{2} \iiint v^2 \rho \, dV = \frac{1}{2} \iiint \nabla\psi \cdot \nabla\Psi \rho \, dV$$

where v is the velocity and ρ is the density. V is the volume. Since Ψ is harmonic, $\nabla^2 \psi = 0$. We use the identity $\nabla \cdot \Psi \nabla\Psi = \nabla\Psi \cdot \nabla\Psi + \Psi\nabla^2\Psi$.

Thus, $\nabla\cdot\Psi\nabla\Psi = \nabla\Psi\cdot\nabla\Psi$. Using the divergence theorem we find,

$$K = \frac{1}{2}\iiint \nabla\Psi\cdot\nabla\Psi\rho dV = \frac{1}{2}\rho\iint \Psi\frac{\partial\Psi}{\partial r}\ r^2 d\mu d\Phi \ . \qquad (2\text{-}24)$$

Since the fluid is incompressible, ρ is constant and it can be brought in front of the integral. From (2-24), using the equation of the spheroid (2-14), we get:

$$K = \frac{1}{2}\rho\iint \Psi\ \frac{\partial\Psi}{\partial r}\ r^2 d\phi d\mu = \frac{1}{2}\rho\iint \Psi\ \frac{\partial\Psi}{\partial r}\ a^2 d\phi d\mu \ . \qquad (2\text{-}25)$$

Here, we neglect the terms containing a_n. The kinetic energy is:

$$K = a^2\pi\rho \int_{-1}^{1} \Psi\frac{\partial\Psi}{\partial r}\ d\mu$$

$$= a^2\pi\rho \int_{-1}^{1} [\beta_o + \sum_{n=1} \beta_n r^n P_n(\mu)][\sum_{n=1} n\beta_n r^{n-1}\ P_n(\mu)]d\mu$$

$$= a^2\pi\rho \int_{-1}^{1} [\beta_o \sum_n n\beta_n r^{n-1}\ P_n(\mu) + \sum_n \beta_n{}^2\ n r^{2n-1} P_n{}^2(\mu)]d\mu \ .$$

The first term will become zero, because of integrating of a single $P_n(\mu)$. Thus,

$$K = a^2\pi\rho\ n\ r^{2n-1}\ \frac{2\beta_n{}^2}{2n+1} \ .$$

Using the equation of the spheroid and neglecting the higher order terms, we get

$$K \approx 2\pi a^2\ \rho n\ a^{2n-1}\ \frac{\beta_n{}^2}{2n+1} \ . \qquad (2\text{-}26)$$

The β_n's are unknown, but we can find them by calculating the velocity of the surface in the r direction from equations (2-1) and (2-23).

$$\frac{dr}{dt} = \frac{da}{dt} + \sum_{n=1} \frac{da_n}{dt} P_n(\mu)$$

$$= \sum_{n=1} \frac{da_n}{dt} P_n(\mu) \qquad (2\text{-}27)$$

$$\nabla\Psi = \frac{\partial\Psi}{\partial r} \vec{U}_r = \sum_{n=1} \beta_n \, n \, r^{n-1} \, P_n(\mu) \quad . \qquad (2\text{-}28)$$

Comparing (2-27) and (2-28), changing r to $a + \sum_n a_n P_n(\mu)$ and neglecting the higher order terms, we get

$$\frac{da_n}{dt} = n\beta_n \, a^{n-1} \quad . \qquad (2\text{-}29)$$

Substituting (2-29) back to (2-26), we get the kinetic energy:

$$K = 2\pi a^3 \rho \sum_n n^{-1} \, (2n + 1)^{-1} \, \dot{a}_n^{\,2} \qquad (2\text{-}30)$$

The Lagrangian function is given by:

$$L = K - P.E. - W$$

$$L = 2\pi a^3 \rho \sum_n n^{-1}(2n + 1)^{-1}\dot{a}_n^{\,2} - 2\pi\gamma \sum_n (n - 1)(n + 2)(2n + 1)^{-1} a_n^{\,2}$$

$$+ \sum_n (n - 1)(2n + 1)^{-1} Q^2 k_1 \frac{a_n^2}{2a^3} \qquad (2\text{-}31)$$

The Lagrangian equation of motion for a_n is

$$\frac{d}{dt}\left(\frac{\partial L}{\partial \dot{a}_n}\right) - \left(\frac{\partial L}{\partial a_n}\right) = 0 \quad .$$

$$\frac{d}{dt}\left(\frac{\partial L}{\partial \dot{a}_n}\right) = \frac{d}{dt}\left(2\pi a^3 \rho \sum_n n^{-1}(2n+1)^{-1} 2\dot{a}_n\right)$$

$$= 4\pi a^3 \rho \sum_n n^{-1}(2n+1)^{-1}\ddot{a}_n \qquad (2\text{-}32)$$

$$\left(\frac{\partial L}{\partial a_n}\right) = -2\pi\gamma \sum_n (n-1)(n+2)(2n+1)^{-1} 2a_n + \sum_n (n-1)(2n+1)^{-1} Q^2 k_1 \frac{2a_n}{2a^3} \quad .$$

(2-33)

Combining (2-32) and (2-33), we get

$$2\pi a^3 \rho n^{-1}\ddot{a}_n + 2\pi\gamma(n-1)(n+2)a_n - (n-1)\frac{Q^2 k_1}{2a^3} a_n = 0 \ ,$$

$$\text{or} \quad \frac{d^2 a_n}{dt^2} + \frac{n(n-1)}{\rho a^3}\left[(n+2)\gamma - \frac{k_1 Q^2}{4\pi a^3}\right] a_n = 0. \qquad (2\text{-}34)$$

This is the familiar result obtained by Rayleigh. If $a_n \propto \cos(wt + \delta)$, then

$$w^2 = \frac{n(n-1)}{\rho a^3}\left[(n+2)\gamma - \frac{k_1 Q^2}{4\pi a^3}\right] . \qquad (2\text{-}35)$$

Thus, if $k_1 Q^2 > 16\pi a^3 \gamma$, the droplet is unstable for all values of n below a criterion limit. The drop may break into smaller drops or, as usual, it may eject a smaller drop carrying charges away to regain stability.

2-3 Determination of the Radius and Charge of the Drop

When a charged waterdrop is levitated at a constant level, the electrostatic force and buoyant force must balance the gravitational force. Thus, we can write the equation: (see figure 2-3)

$$\frac{4}{3}\pi R^3(\rho_w - \rho_a)g = Q\,E_b, \tag{2-36}$$

where R is the radius of the drop,

ρ_w is the density of the water, 10^3 kg/m^3,

ρ_a is the density of the air, 1.293 kg/m^3,

g is the acceleration of gravity, 9.81 m/sec^2 in Thunder Bay,

Q is the charge on the drop, and

E_b is the balanced electric field.

Since $\rho_a << \rho_w$, we set $\rho_a = 0$ in equation (2-36).

If we suddenly reduce the electric field, the drop begins to fall. The force acting on the falling drop are the gravitational force, the reduced electric force and Stokes' force. (See figure 2-4.) Using Newton's Second Law, we obtain the equation of motion:

$$\frac{4}{3}\pi R^3 \rho_w \frac{dV}{dt} = -\frac{4}{3}\pi R^3 \rho_w g + QE_r - 6\pi\eta RV, \tag{2-37}$$

where V is the velocity of the drop,

η is the viscosity of the air, 182.7×10^{-7} kg/msec, and

E_r is the reduced electric field.

Calculating the charge Q from equation (2-36), we get

$$Q = \frac{4}{3}\pi R^3 \rho_w g E_b^{-1}\ . \tag{2-38}$$

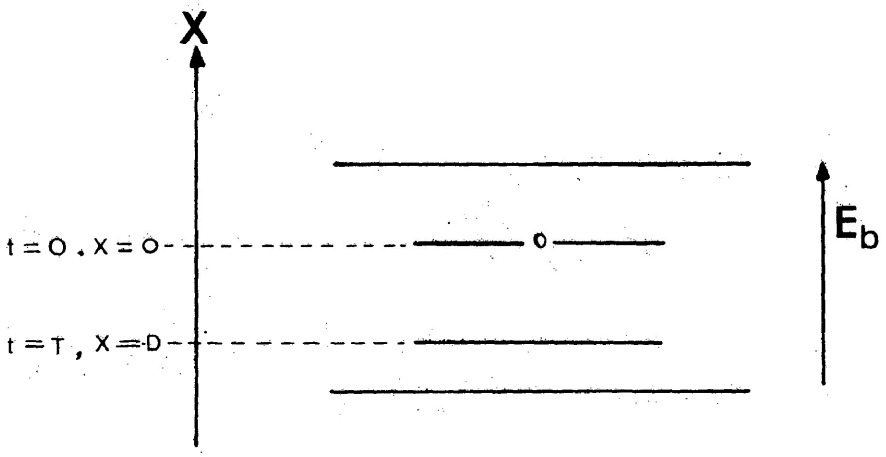

Fig. 2-3 Motionless charged drop levitated by the electric field

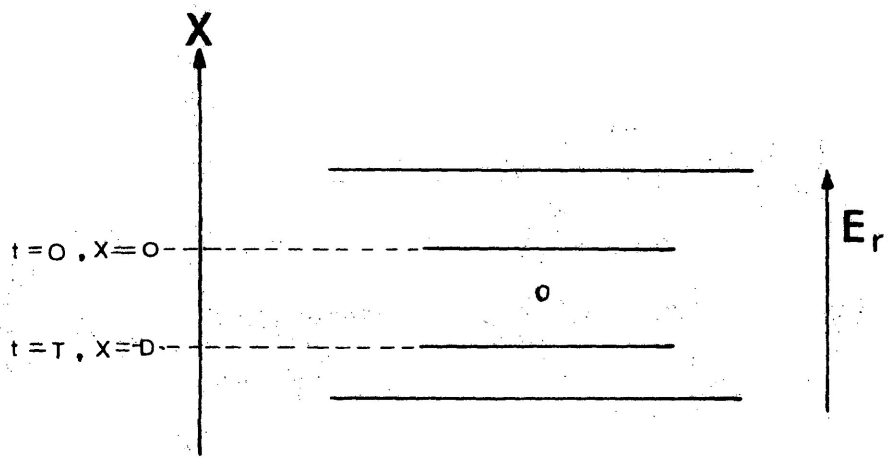

Fig. 2-4 Charged drop falling under reduced electric field

Substituting (2-38) back into (2-37), we get

$$\frac{4}{3}\pi R^3 \rho_w \frac{dV}{dt} = -6\pi\eta RV - \frac{4}{3}\pi R^3 \rho_w g + \frac{4}{3}\pi R^3 \rho_w g \frac{E_r}{E_b}$$

$$\frac{dV}{dt} = -\frac{9\eta}{2\rho_w R^2} V - g\left(1 - \frac{E_r}{E_b}\right).$$

Let $A = \frac{9\eta}{2\rho_w R^2}$, $B = g\left(1 - \frac{E_r}{E_b}\right)$. We get,

$$\frac{dV}{dt} = -AV - B \ . \qquad (2\text{-}39)$$

The solution of (2-39) is:

$$V = -\frac{B}{A}\left(1 - e^{-At}\right) \qquad (2\text{-}40)$$

$$X = -\frac{B}{A} t + \frac{B}{A^2}\left(1 - e^{-At}\right) \qquad (2\text{-}41)$$

when $t = T$, $x = -D$, so

$$D = \frac{B}{A} T - \frac{B}{A^2}\left(1 - e^{-AT}\right). \qquad (2\text{-}42)$$

Let us estimate the number AT. Suppose the radius is 60 μm (60×10^{-6} m), and the falling time is 5.4 sec.

These numbers are taken from experimental results.

$$AT = \frac{9 \times 182.7 \times 10^{-7}}{2 \times 36 \times 10^{-7}} \times 5.4 = 123 \ .$$

Thus, the number e^{-AT} actually is very small. We can drop this term in the equation (2-42). The simplified equation is

$$D = \frac{B}{A} T - \frac{B}{A^2}$$

$$(\frac{1}{A})^2 - T(\frac{1}{A}) + \frac{D}{B} = 0$$

$$\frac{1}{A} = \frac{1}{2} T \pm \frac{1}{2} \quad (T^2 - 4\frac{D}{B})^{\frac{1}{2}} \qquad (2\text{-}43)$$

Substituting the values of A and B back into the equation (2-43), we get:

$$R^2 = \frac{9\eta}{4\rho_w} [T \pm (T^2 - \frac{4D}{g(1 - \frac{E_r}{E_b})})^{\frac{1}{2}}]$$

$$= \frac{9\eta}{4\rho_w} [T \pm T (1 - \frac{4D}{g(1 - \frac{E_r}{E_b})T^2})^{\frac{1}{2}}].$$

In this experiment, E_r is chosen 97.5% of E_b. The distance of fall is 5 cm. In a typical case, the falling time is 5.4 sec. The value of $\frac{4D}{g(1 - \frac{E_r}{E_b})T^2}$ is approximately 0.028, which is small compared to 1. Using the binomial theorem and choosing the negative sign in the equation, we get:

$$R^2 = \frac{9\eta}{4\rho_w} (\frac{2D}{g(1 - \frac{E_r}{E_b})T}) \qquad (2\text{-}44)$$

This equation can also be obtained by assuming that the drop falls the whole distance D at terminal velocity.

We now have the result that the radius and charge of the drop can be determined from equations (2-44) and (2-38):

$$R^2 = \frac{9\eta}{4\rho} \left(\frac{2D}{g\left(1 - \frac{E_r}{E_b}\right) T} \right) \qquad (2\text{-}44)$$

$$Q = \frac{4}{3} \pi R^3 \rho_w g E_b^{-1} \qquad (2\text{-}38)$$

3. APPARATUS

3-1 Main Description

The apparatus is designed to produce fine waterdrops and built embodying the principle of the Millikan (1935) oil-drop experiment (figure 3-1). The whole apparatus sits inside a vacuum evaporator* on the top of 2.54 cm thick aluminum plate, covered with a glass jar 17.78 cm in radius and 60.96 cm in height. The purity of water used in the experiment may be an important factor, so filtered distilled water was used. The method for producing fine water drops by the vibrational method, based on the device of B. J. Mason, O. W. Jayaratne and J. D. Woods (1963), will be described in detail in the next section. The vertical electric field required to levitate the waterdrops is applied by two parallel aluminum plates 15.24 cm in radius and 1.77 cm in thickness. The plates are polished smoothly and rounded at the edge to provide a moderately uniform electric field at the centre.

In the center of the top electrode, a small hole is drilled to let the drops fall into the field region. A gate device which can be closed immediately after a suitable drop is chosen sits on the top electrode. It is a movable aluminum plate connected to a solenoid and powered by three 6-volt batteries connected in series. (See figure 3-2.)

The distance between the bottom plate and the lower electrode, the distance between electrodes, and the distance between the top electrode and the Plexiglas plate where the vibrational apparatus sits are 15.24 cm, 11.43 cm and 12.70 cm respectively; Plexiglas rods of

*The major components are shown in table 3-1.

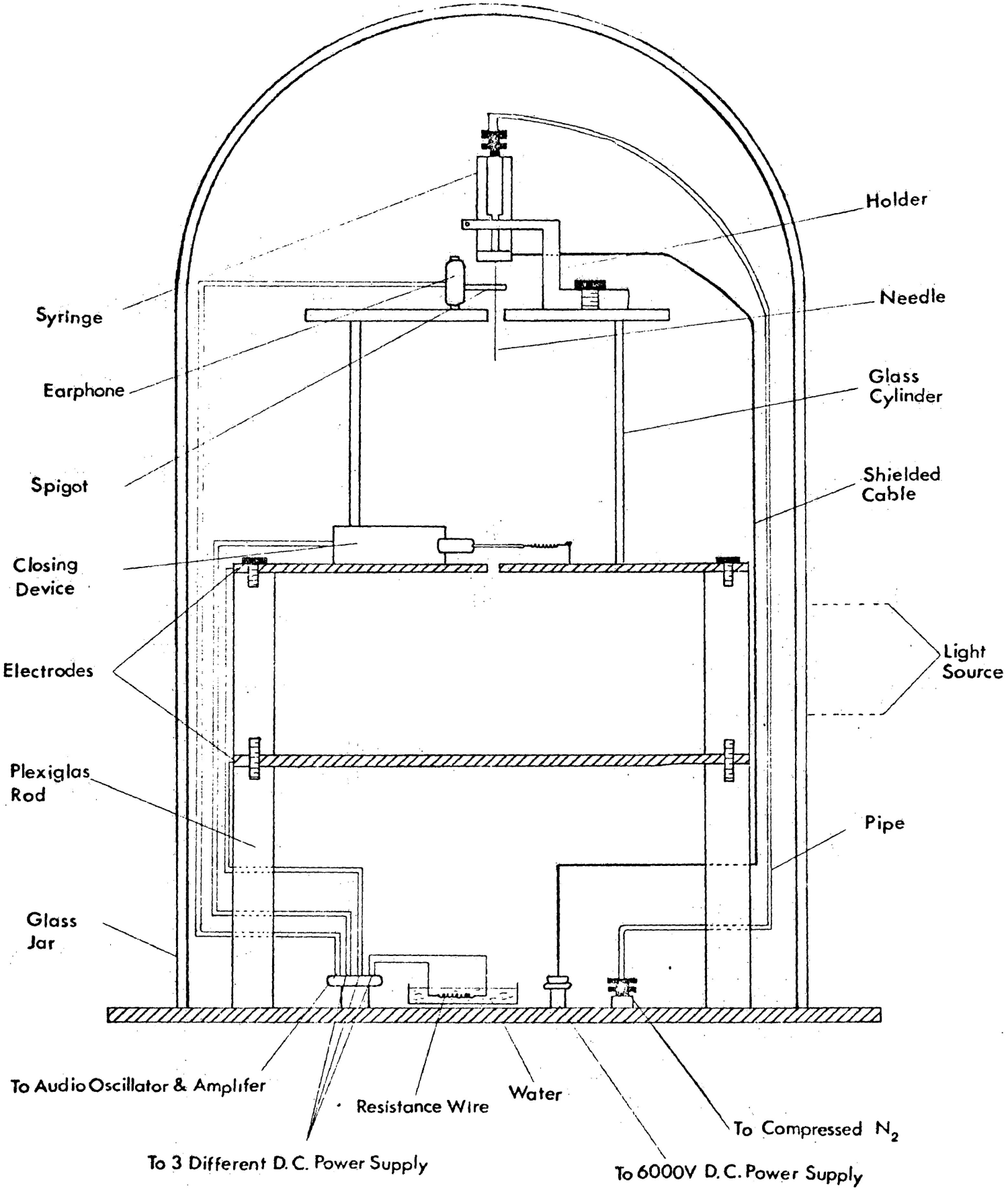

Fig. 3-1 General view of experimental apparatus

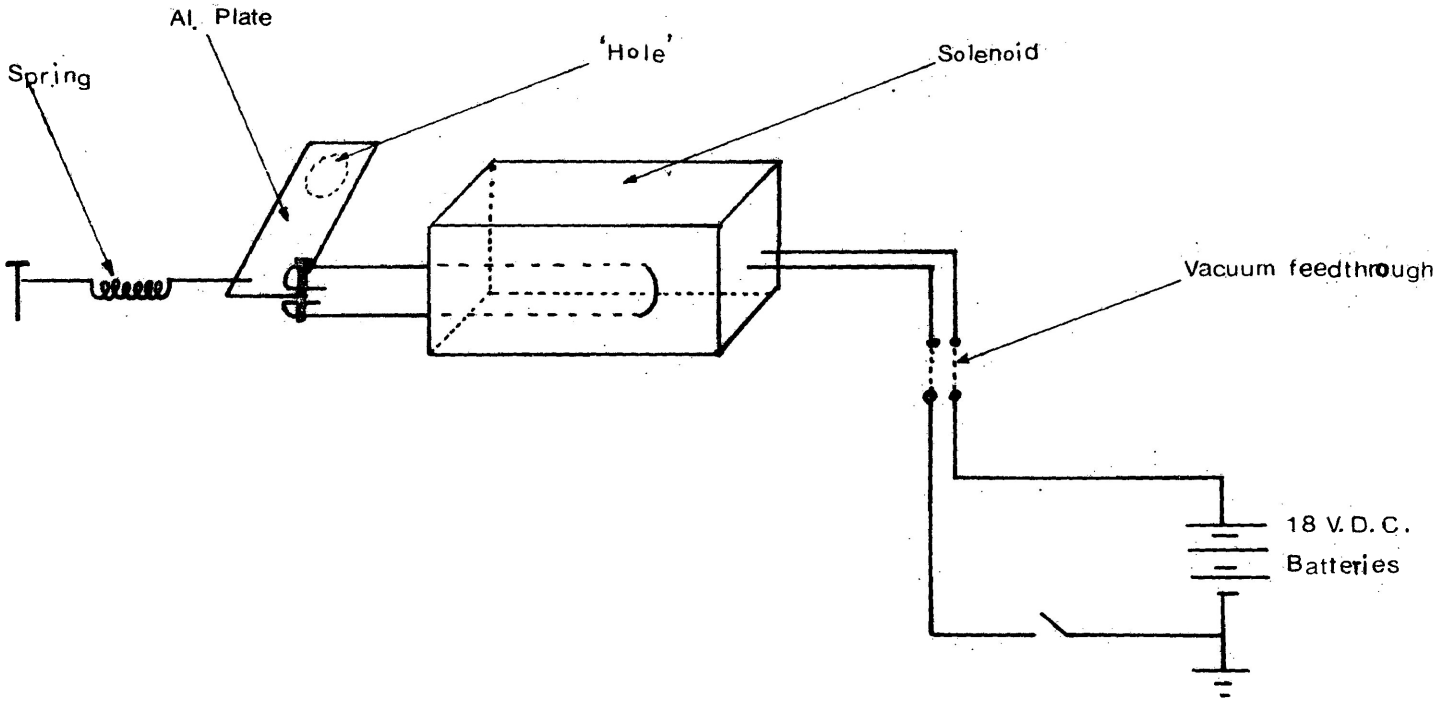

Fig. 3-2 Gate for closing hole in top electrode

TABLE 3-1 Major Components of Apparatus

Component	Manufactured by	Model
Evaporator	NRC	3114
600V D.C. Power Supply	Hewlett Packard	712 C
Digital Voltmeter	Fairchild	7050
6 KV D.C. Power Supply	Sorensen	9005-5
Recorder	Bausch & Lomb	VOMT
Transformer	Leybold	591 05
Compressed N_2	Canadian Liquid Air	'G'
6 Volt Battery	Eveready	

1.77 cm radius are used for support.

A continuously variable voltage is applied across the electrodes from a D.C. power supply. The field voltage is measured by a digital voltmeter. The waterdrops are charged by another D.C. variable power supply. The cable connecting this high voltage and needle is shielded and grounded to prevent any affect on the electric field. The inside of the glass jar is shielded with a grounded aluminum foil to prevent electrostatic effects on the electric field or the drops. Black conducting paper is placed over the foil to provide better viewing. Two holes are left in the foil; one for the light to enter, the other for viewing. The light source used in this experiment is a 500 Watt projector lamp with a heat filter made of glass box containing cupric chloride solution. The purpose of the heat filter is to reduce the heating effect of the light on the air inside the jar and on the drop itself. Nevertheless, some convection currents were still present. A resistance wire was used to heat water in a glass vessel to increase the humidity inside the glass jar.

The first vacuum feedthrough at the left in figure 3-1 is an electrical connection. It has 8 connecting points. Numbers 1 and 4 are connected to the electrodes and a 600 V D.C. power supply. Numbers 2 and 3 are connected to the earphone (described in the next section) and audio oscillator. Numbers 6 and 7 are connected to the solenoid and batteries. Numbers 5 and 8 are connected to the resistance wire and transformer. The second feedthrough is for high voltage. It allows the needle to be connected to a 6 KV D.C. variable power supply. The last one is a pipe connection joining the syringe and compressed

nitrogen used to control the flow rate through the needle.

3-2 Production of Fine Waterdrops by a Vibration Method

3-2-1 Introduction

The most successful method of producing fine waterdrops of radii in the range of 15 μm to 500 μm involves the break up of a mechanically vibrated jet of liquid, the theory of which was given by Rayleigh (1879). Some other ways have been used; for example, an electromechanical transducer to introduce pressure fluctuations directily into the liquid prior to its emergence as a jet. However, if a uniform, stable flow is needed, the best way is still the vibration method.

Dimmock (1950) first designed a vibrating device based on the principle of Rayleigh. The device is capable of producing fine drops, but it is very difficult to obtain reproduciable and stable modes of vibration and the sizes and directions of the streams are variable and difficult to control.

In 1960, Schotland reported that he had used a vibrating hypodermic needle to produce drops in the radius range 150 to 500 μm, but his paper gives no experimental details.

The apparatus used in our experiment is based on the device of B. J. Mason, O. W. Jayaratne and J. D. Woods (1963). The purpose of their work was to produce a device to study the collision and coalescence of small waterdrops. It has proved to be useful also in the production of fine waterdrops for evaporation. The device produces directed streams of waterdrops of very uniform size with radii in the required range.

3-2-2 Construction and Operation

A general view of the device is shown in figure 3-3. The holder of the syringe* and earphone** is made of Plexiglas. The earphone part is fixed, but the syringe part is adjustable, the needle going right through the hole in a spigot.*** The position of the needle may be adjusted by changing the holding position of syringe. More details of the construction are shown in figure 3-4. A stainless steel tube of 101.6 μm inside diameter and 203.2 μm outside diameter, through which water is forced at a constant rate, fits snugly into a small central hole near one side in the cylindrical spigot, which is cemented to the center of an iron diaphragm of an electromagnetically driven earphone. The energizing coil of the electromagnet is connected to an audio oscillator and power supply which causes the needle to be vibrated mechanically by the movement of the diaphragm and spigot. The frequency of the oscillator is adjusted until a resonant mode is reached with an amplitude of several millimeters. The resonance frequency which is quite sharply defined is determined not only by the needle, but also by the size and mass of diaphragm and spigot. For example, in this experiment a 7.5 cm long, 101.6 μm inside diameter tube driven at a point 5 cm from its tip resonates at about 310 Hz, a change of ± 10 Hz being sufficient to damp the oscillation completely. To ensure that the needle vibrates in the same stable mode for long periods, it is

* The syringe is made of Plexiglas, 0.76 cm in radius, 6.43 cm in length.
** The earphone is made by C. F. Connon Co., Springwater, New York, Brand: Alnico Magnet No. 25.
*** The spigot is made of Plexiglas, 0.37 cm in radius, 1.90 cm in length.

Scale : 1 : 2

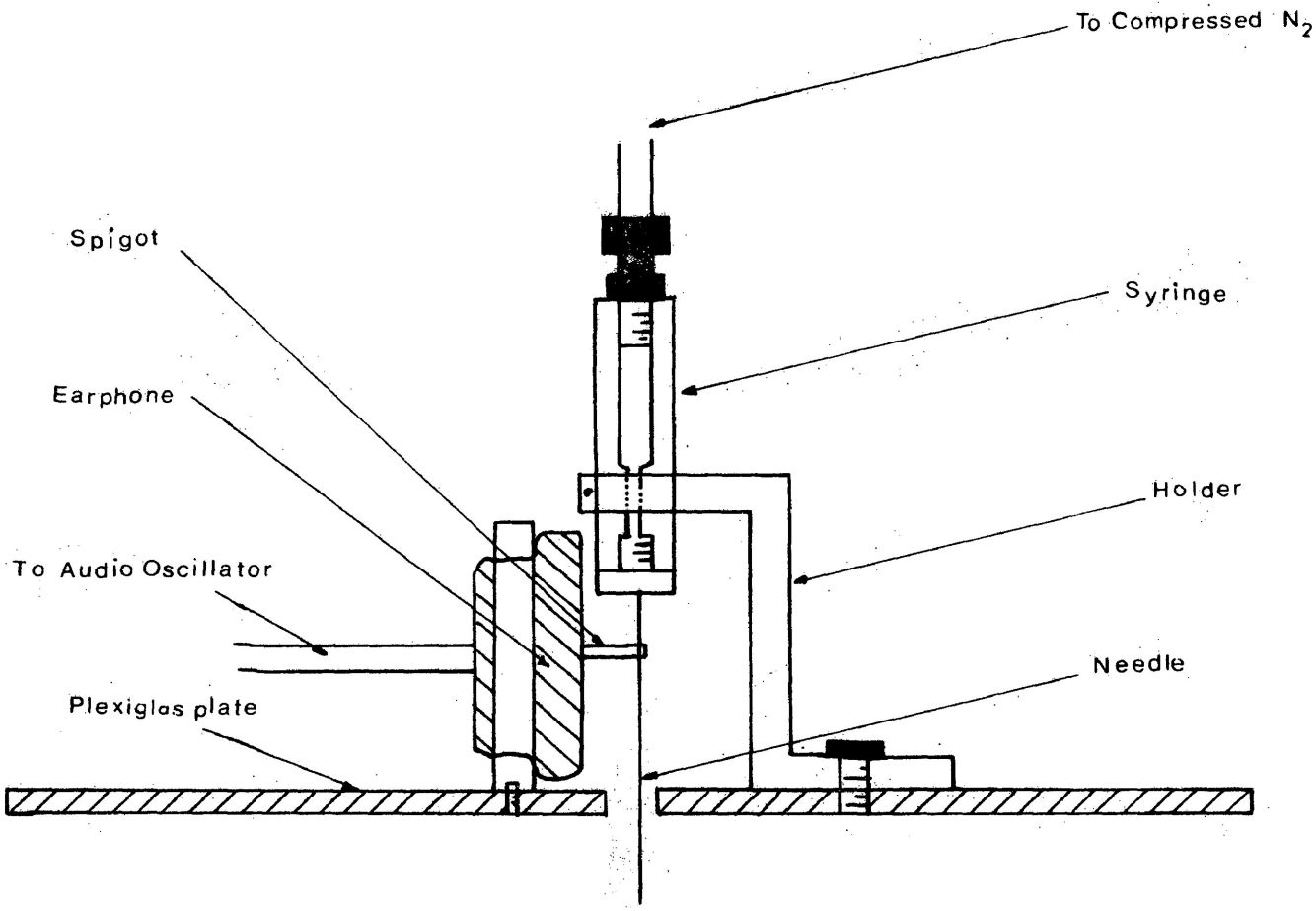

Fig. 3-3 Vibrating needle for producing charged drops

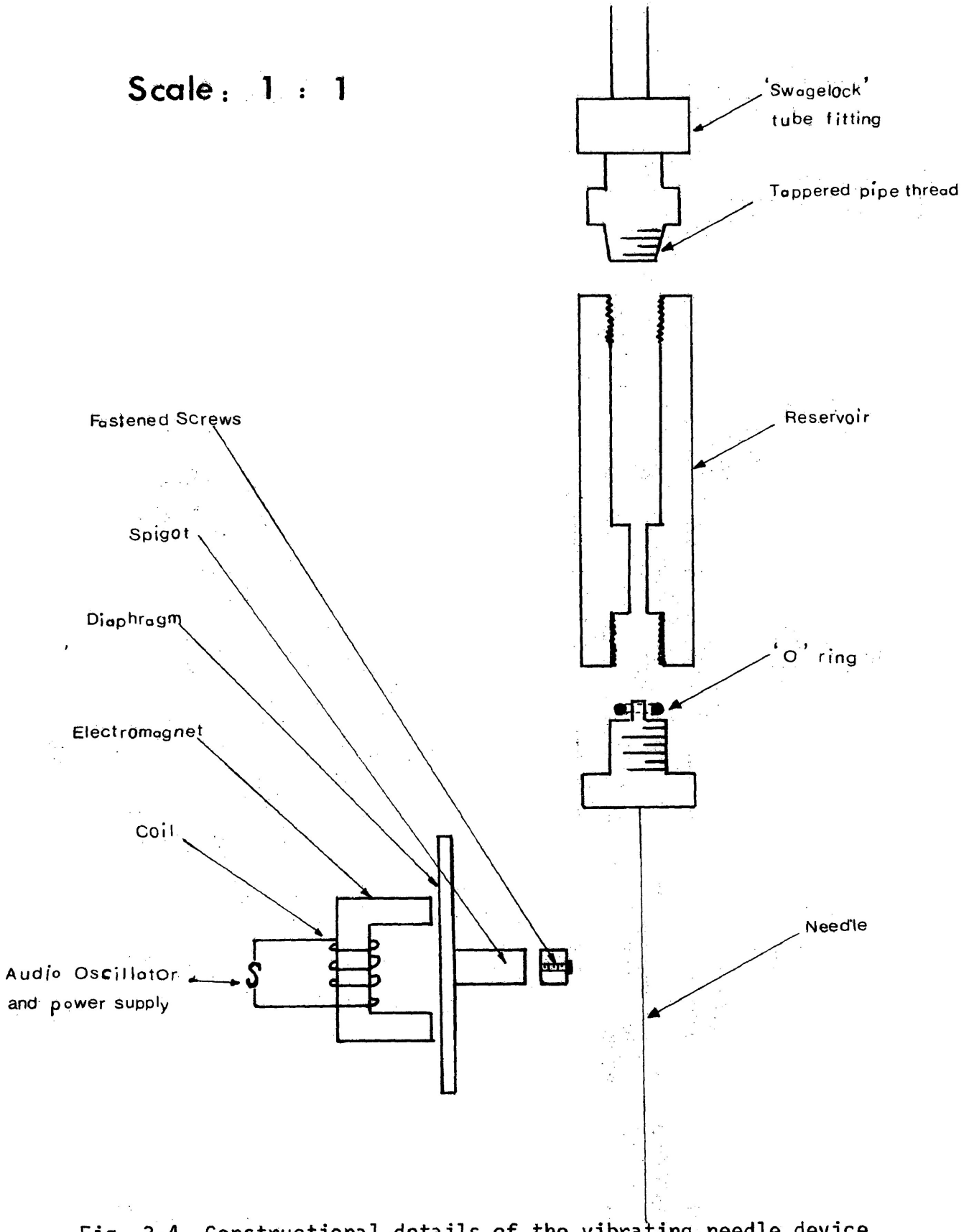

Fig. 3-4 Constructional details of the vibrating needle device

necessary to prevent it from moving in the spigot; this is achieved by the small locking screw at the end of the spigot.

The stability of the droplet stream is particularly dependent upon the flow rate of the water and it is essential to keep this constant. The water is forced from the reservoir by the compressed nitrogen. The nitrogen supply is maintained at constant pressure controlled by the regulator. A needle valve and 'T' tube connection are placed between the nitrogen and syringe for releasing the pressure when not in use.

For a given needle and amplitude, a critical volume of water has to accumulate before it is flung off by a change in direction of the needle. At low flow rates the needle may vibrate several times before the critical volume of water accumulates; there is a tendency to eject this as a single drop. As the flow rate is increased, the water comes out continuously and breaks up into small masses. After travelling about 1 cm, the drops assume a spherical shape. Drops of different sizes are projected in different directions and produce separate streams, the number of which may also be controlled by the frequency and amplitude of the vibrations. The needle used in this experiment is quite long, so the pressure change in the compressed nitrogen does not greatly affect the flow rate. This is very helpful in keeping the flow rate constant.

If the needle vibrates in one plane, the major and satellite streams are almost coplanar but, more usually, the tip vibrates in a circle, an ellipse or a figure of eight. Then the droplets are flung off in different directions.

3-2-3 Control of Droplets' Size and Frequency

The main factors determining the size of droplets are the flow rate of water (mentioned in section 3-2-2), needle diameter, the resonant frequency and the amplitude of vibration.

(a) Needle tip diameter

A 101.6 μm inside diameter stainless steel tube is used as the needle. It is chamfered 30^{0} to produce the drops. The needle is long enough (7.62 cm) to dampen flow rate charges at the tip under the inevitable fluctuating pressure. If drops of different radii are needed we just change the tube to a larger size.

(b) Resonance frequency

The resonance frequency depends on the length of the needle, the position where the spigot is driven and the mass of spigot and diaphragm. It is very critical, so usually it takes time to find out the frequency, especially if the position of the spigot position is changed. The range is of the order of ± 20 Hz at 300 Hz.

(c) Amplitude of Vibration

It is often convenient to fix all the other factors and to vary the droplet size slightly by adjusting the output amplitude of audio oscillator and hence the amplitude of the needle oscillation.

3-2-4 Production of Highly Charged Droplets

When a highly charged droplet is needed, a 6 KV variable D.C. power supply is connected to the needle. The drops split when about 5 KV is applied and produce drops of radius 200 μm even without vibration. If vibrated, the needle will produce highly charged drops of 15 μm radius or even smaller.

3-2-5 Conclusion about the Vibration Method

The vibration method is very useful for the production of droplets in the range of 15 μm to 200 μm needed in this experiment. There is still one drawback which arises from the change in the position of the spigot when the reservoir is refilled, necessitating a slight adjustment of the frequency each time.

3-3 Field and Time Control

The method of measuring the radius and charge involves reducing the electric field suddenly and then determining the time for the drop to fall through a fixed distance. The ratio of reduced field to the original field should be a fixed number. A small potentiometer is used as shown in figure 3-5. A double pole switch and two resistors, R1 and R2, are kept in a small box work as a potentiometer. The values of R1 and R2 are 1.02×10^7 Ω and 1.45×10^5 Ω respectively. When the reduced field is required, the potentiometer is switched in and the voltage is reduced to the 97.5 percent of the original balanced voltage. Simultaneously, the other side of the switch is shorted, so the timer starts to record the time until the switch is released. This small potentiometer thus provides an automatic time recorder. A precision digital voltmeter is placed across the electrodes so that it will give both the balanced voltage and the reduced voltage. A recorder is placed in parallel to the 600 V D.C. power supply so that it will record the voltage as a function of time during the measurement.

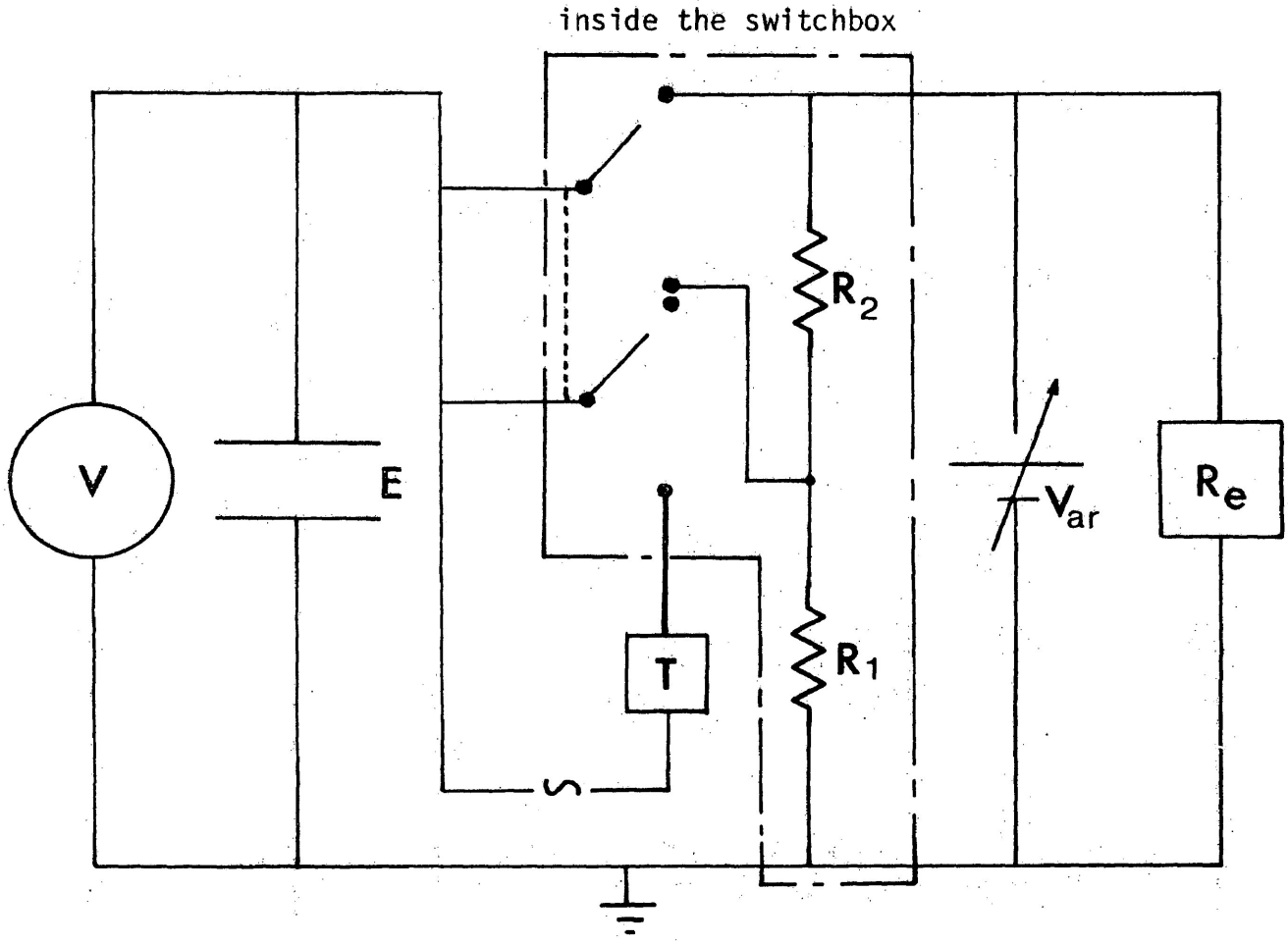

V : Voltmeter
E : Electrode
T : Timer
R_2 : Small resistor
R_1 : Large resistor
V_{ar} : Variable D.C. power supply
Re : Recorder

Fig. 3-5 Diagram of circuit for reducing the electric field

4. MEASUREMENTS

4-1 Procedure of Measurements

Small charged waterdrops are produced as described in section 3. The hole on the top electrode is opened by controlling the solenoid, with the result that the drops fall under gravity and enter the illuminated field. A suitable drop is chosen by adjusting the potential difference between the horizontal electrodes; it can be manipulated so that it remains in the field. The top hole is then closed to prevent more drops coming in; all other drops residing between the field will soon drift out of the field since their charge to mass ratio will in general differ from that required for levitation. This is the well-known Millikan method. (See figure 2-3.) The charge and radius of this drop are determined every 30 seconds. Two measurements are required. One is the electric field needed to suspend the drop so that it is motionless. The other is the time necessary for the drop to fall a distance D in the reduced field E_r. This reduced field is obtained by means of a switch as discussed in section 3-3. The distance of fall is marked by two lines drawn on the viewing window and two other lines drawn at the same level on the other side of a glass jar. This prevent parallax during measurement. It is hard to get accurate timing. The uncertainty is large, but it is still possible to know the radius of the drop within ± 10%. The field required to suspend the drop before the disintegration occurs decreases gradually and continuously as the evaporation proceeds. Evaporation thus produces an increase in the charge to mass ratio of the drop. When a disintegration happens, the drop falls quickly and the field strength must be increased abruptly in order to retain the residual droplet between the electrodes.

With some practice it is possible to suspend a droplet throught a succession of disintegrations. Each disintegration is accompanied by a loss of about 20% to 30% of the charge residing on the droplet. The mass loss in a disintegration is around 20%. No measurable loss of charge occurs during the intervals between successive disintegrations, but the radius decreases continuously in these periods.

5. SOME DIFFICULTIES IN THE EXPERIMENT

5-1 The Drops

When the needle vibrates, the drops are thrown about 7 cm horizontally away from the needle. (See figure 5-1.) This distance depends on the frequency and output of the audio-oscillator. If we put a high voltage on the needle and thus charge the drops, they are thrown even further. (See figure 5-2.) If we want the drops to fall vertically into the electric field, we need to put the needle about 12 cm away from the centre. (See figure 5-3.) Because of the narrow space inside the glass jar (35.56 cm in diameter and 60.96 cm in height), it is hard to put the needle in this position.

To solve this problem, I tried many methods. First, I tried to put a high voltage ring around the needle to produce a field to change the direction of the drops by electrostatic repulsion. Second, I tried to put a ring carrying a small voltage around the centre hole to attract the drops. Third, I tried to produce a strong non-uniform field to charge the drops and then use a small field to attract the drops falling vertically through the hole. However, the more fields I used, the more complicated the situation became and the more difficult it was to control the drops. Finally, I solved the problem by using a big glass cylinder to support the whole vibrating apparatus, with the needle a little off the center. (See figure 5-4.) When the drop charging is initiated, some of the drops are repelled by the first few drops that land on the glass and then fall through the hole. The drop size could be controlled by changing the output of the audio

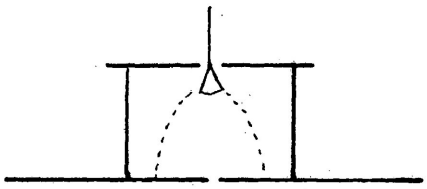

Fig. 5-1 Uncharged drops are thrown about 7 cm away from centre hole

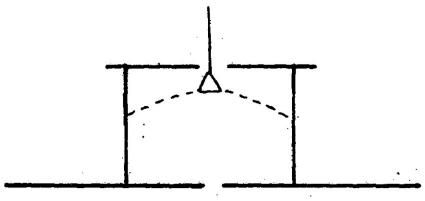

Fig. 5-2 Charged drops are thrown even farther

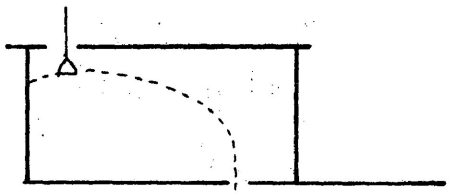

Fig. 5-3 Ideally the drops can fall into the electric field vertically

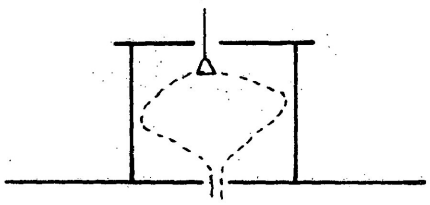

Fig. 5-4 The drops are repelled by the glass wall and pass through the hole

oscillator, that is, changing the amplitude of the needle vibration. (See section 3-2-2 (c).) Sometimes, I could even select the number of drops falling into the field. That had the advantage of avoiding too many highly charged drops falling into the field at the same time, causing a strong mutual repulsion.

5-2 The Field

The uniformity of the levitating field for suspended drops is important. A small degree of irregularity causes the drops to drift, sometimes to the point where they cannot be controlled at all. To counteract this tendency, the electrode (30.48 cm in diameter, 0.635 cm in thickness) is made as smooth as possible with a flat inside plane but some unevenness still remained (± 0.005 cm). The grounded foil on the glass jar affects the field, especially at the edge. (See figure 5-5 a,b). But, if we always keep the drops at the centre part of the field, the effect is very small. The hole in the top electrode affects the field also, but it was made as small as possible to avoid serious distortion of the uniform field. The drop is usually suspended about 3 cm away from the top electrode, so the effect of that hole probably is very small (less than 0.1% of the field).

5-3 The Evaporation Rate of the Drop

The evaporation rate of the drop depends on the ambient temperature, the humidity inside the glass jar, the temperature of air circulating inside the room, the absorption of heat from the illuminating device, and the initial temperature of the drop.

Because the volume of the drop is small, the force exerted on it is small too. A 70 μm radius drop experiences a gravitational force of 1.41×10^{-8} N. Thus, some small factors which are normally

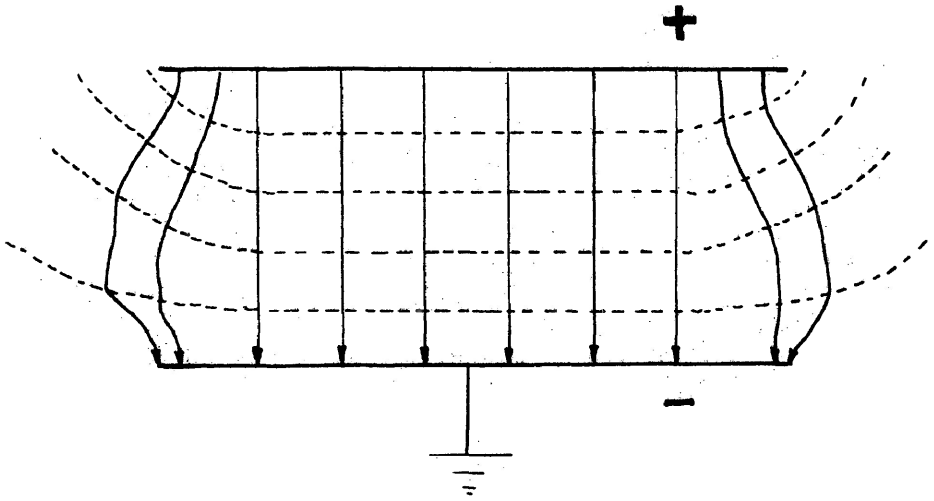

Fig. 5-5a The shape of the electric field without grounding foil

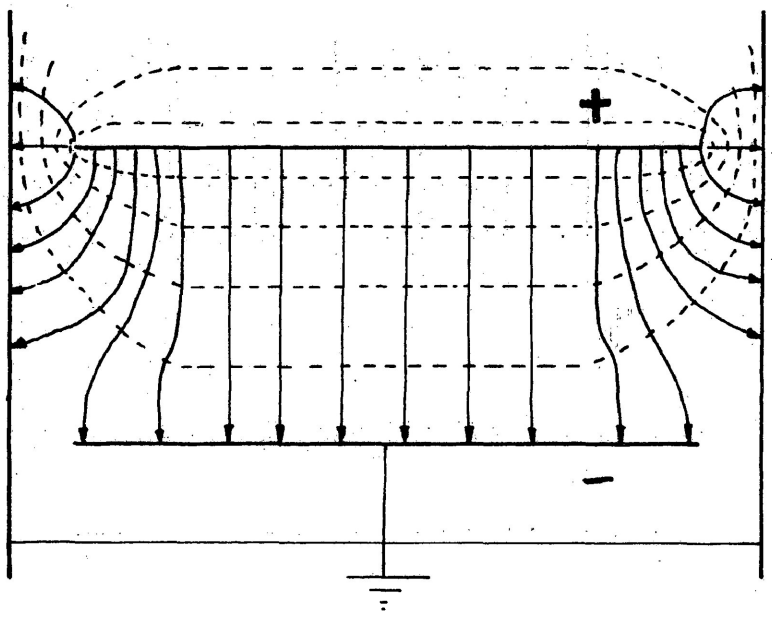

Fig. 5-5b The shape of the electric field with grounding foil

——— Electric field lines
--------- Equipotential surface

neglected must be considered carefully in this experiment. The heat transferred from light is one. The projector used in this experiment produces a wide spectrum, and the absorption of water is different for different wavelengths. A heat filter is used, made of cupric chloride solution contained in a glass container (7.62 cm in diameter and 15.24 cm in length). The efficiency of this heat filter has not been tested accurately, but nearly two-thirds of the heat is removed: this figure was derived from a crude measurement using a precision thermometer. The distance between the projector and the drop is a factor also. Usually, the distance is around 200 cm. In a sub-experiment, a higher evaporation rate was found when the distance was reduced to 60 cm.

The fluctuation of room temperature, which is poorly controlled, is probably the biggest factor in the evaporation rate of the drop. When the room temperature is increasing, the evaporation rate increases markedly. Even just a few degrees Celsius change in the room temperature affects the evaporation rate almost immediately. To solve this difficulty, the temperature is recorded continuously and the experiment is always performed at a time of stable temperature. Extreme circulation of air in the room was prevented by blocking the outlet of the ventilating system. A decreasing temperature helps the drop last longer; that is, it causes a lower evaporation rate. This effect could not be accurately measured with the equipment at my disposal.

A high humidity inside the glass jar causes a lower evaporation rate also. In the beginning of this experiment, much time was wasted because the humidity inside the jar was low. I tried to run the experiment right after I closed the glass jar, but failed to catch the drops. The drops moved very rapidly and disappeared. It took a great deal of patience

to discover the reason. After I put a vessel of warm water into the jar and left it overnight, the situation became somewhat better. I was able to catch and control the drops. The humidity is now raised by heating water inside the glass jar with a low-voltage resistance wire. After 20 minutes or so, high humidity is reached and water condenses on the glass jar. The current is then switched off and the system is left overnight to reach equilibrium.

5-4 Some Difficulties in the Measurement

The drop size is small, usually around 70 μm. It is very hard to look at the drop in the field even though the background in the jar and room is darkened. Thus, it is necessary to relax the eyes after each measurement.

The position of the drop is judged by the eye, so uncertainty is involved, especially when the falling velocity is fast. Parallax causes some uncertainty too. The uncertainty is discussed in section 6.

Great care was taken to determine the balanced field precisely. This is important since the whole measurement depends on only a 2.5% reduction of this field.

If the evaporation is fast, it is impossible to measure the size of the drop. Since the drop must fall for at least 3 seconds through the vertical measuring distance, the measurement will be inaccurate if the radius changes appreciably in this time. Sometimes it is necessary to reduce the field continuously to balance the drop, since it is evaporating. At times, the drop does not fall, or it falls a small distance and then rises up again, when the field is reduced. Details of this are discussed in section 6.

As mentioned at the beginning, the size of the drop is small. Thus, when I do this experiment I must concentrate on controlling the drop in the field. I cannot record the voltage of the balanced field and the time of the fall as well. A TV camera was used to take pictures of the timer and digital voltmeter. The data was recorded on video tape so that it could be examined after several drops were processed.

6. RESULTS AND DISCUSSION

6-1 Results

From Rayleigh's criterion, we may expect that:

$$k_1 Q^2 < 4\pi(n + 2)R^3\gamma \qquad (6\text{-}1)$$

where γ is surface tension, n is an integer greater than or equal to 2. During the progress of this experiment, approximately 100 different drops were examined.

First, we look at the results for the negatively charged drops. From figure 6-1, which plots the radius, charge and critical function against time, we can see a typical result of the experiment. (Exact data are shown in Table 6-1 and a sample calculation is shown in Appendix III.) From the top we see that the radius of the drop R decreases continuously, until a disintegration happens; the radius loss is about 6.22% This corresponds to 17.53% loss in mass. From the middle graph we see that the charge always keeps constant, until the disintegration happens with a loss of 19.4% of charge. From the bottom graph we see that the critical function increases and reaches its highest value at the disintegration point. After the disintegration, the value of the critical function becomes lower, the drop becoming more stable. But, after a few seconds, another disintegration happens and the mass loss is large, so that the drop hits the bottom electrode before the field can be increased. Figures 6-1a, 6-1b and 6-1c show the radius, charge and critical function vs time in large scale graphs.

Now we consider the positively charged drops. Figure 6-2, which plots the radius, charge and the critical function against time, shows a typical result. Exact data are shown in Table 6-2. There is

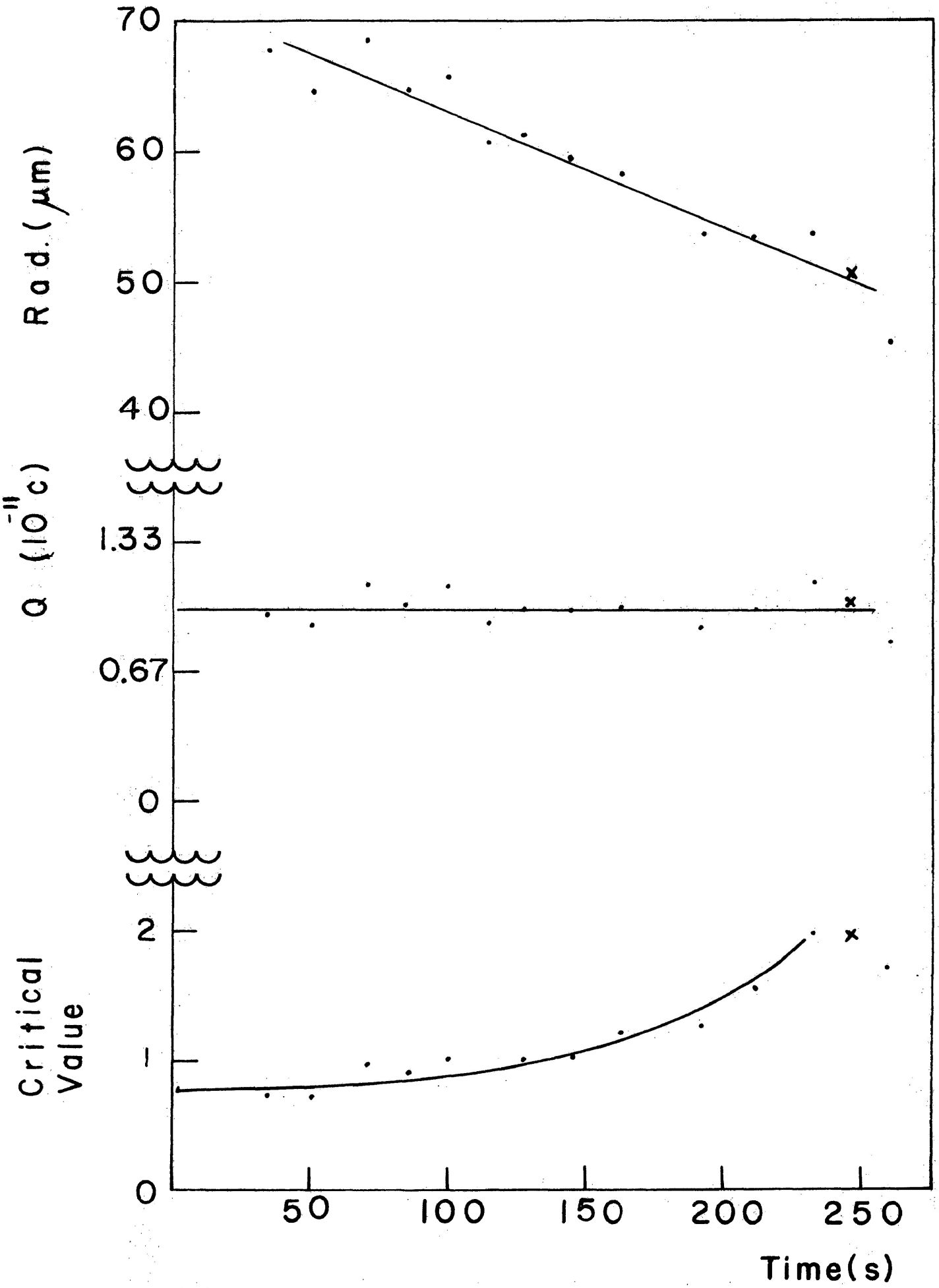

Fig.6-1 Radius, charge and critical value plotted against time for a typical negatively charged drop
× : First disintegration point

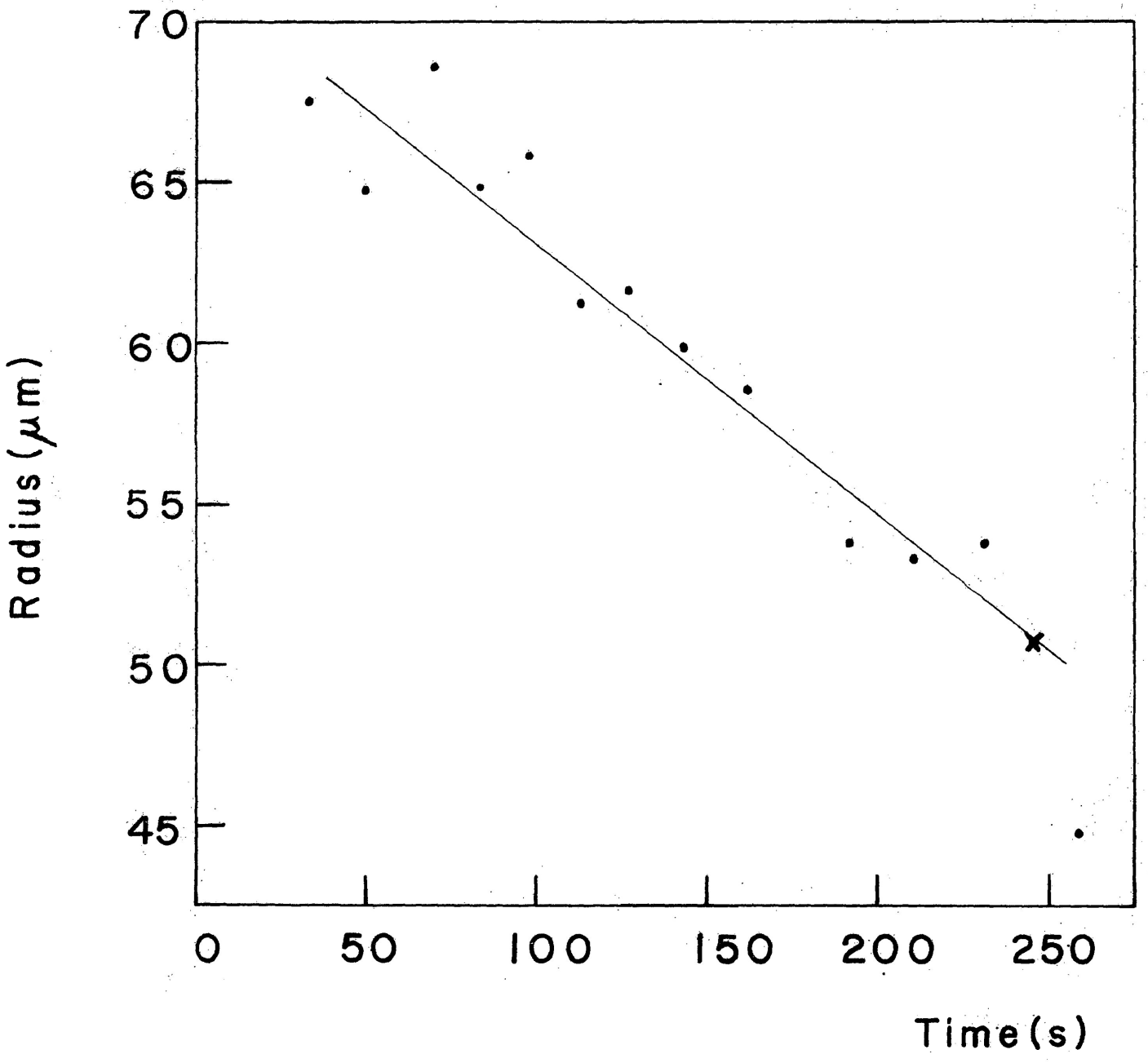

Fig. 6-1a Graph of Radius vs Time (NEGATIVE)
x: Disintegration Point

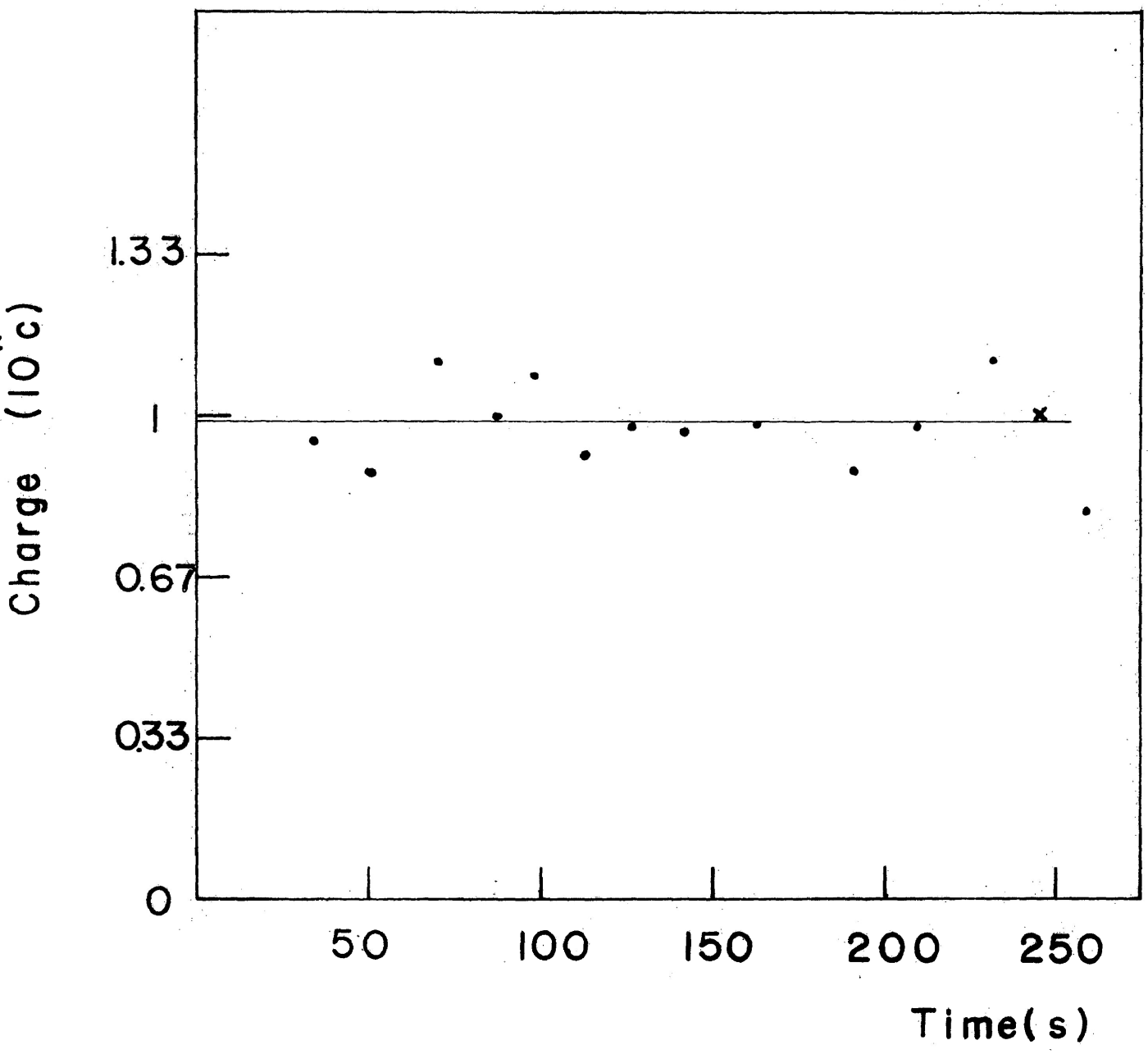

Fig. 6-1b Graph of charge vs. time (NEGATIVE)

X: Disintegration point

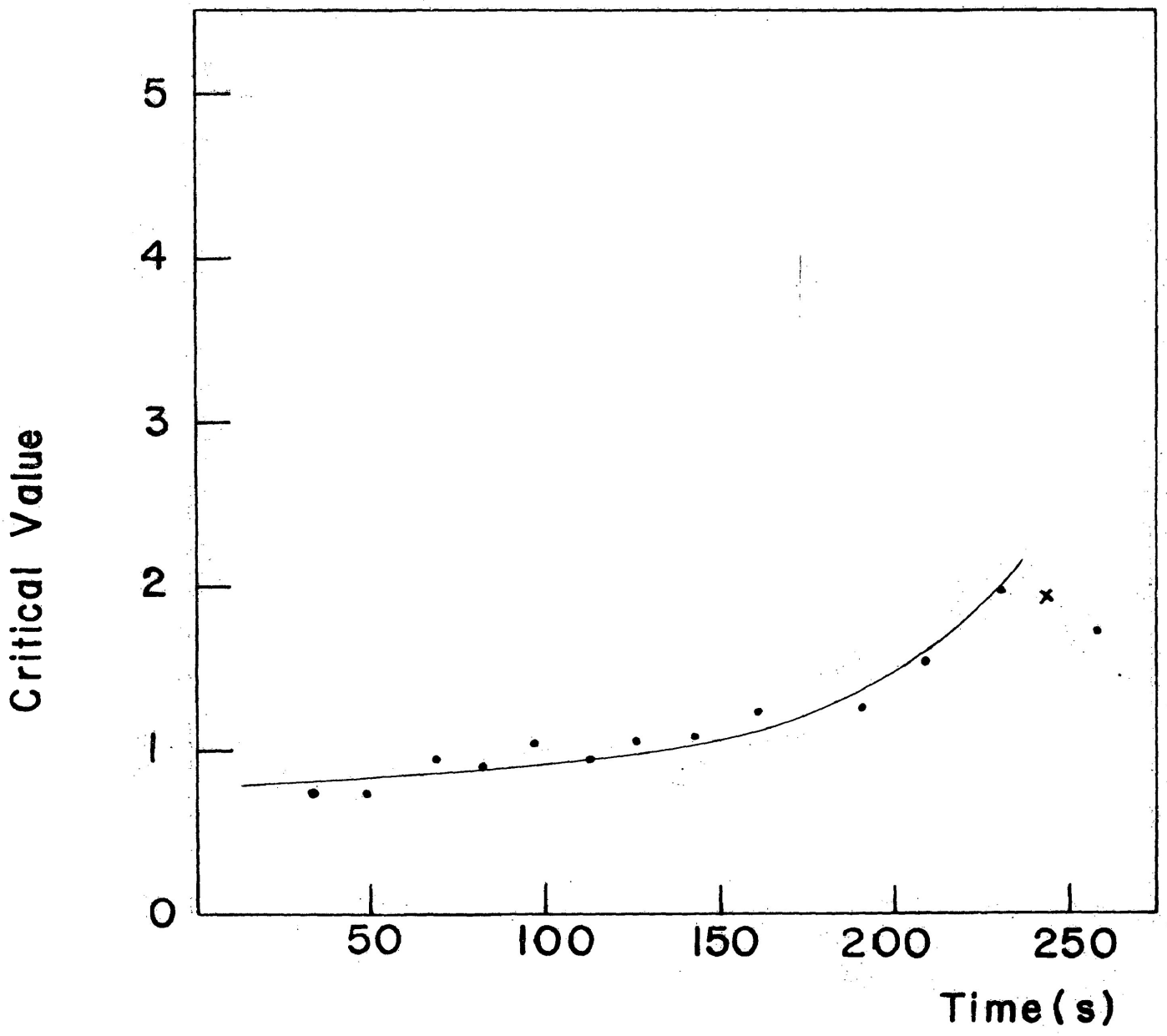

Fig. 6-1c Graph of critical value vs. time (NEGATIVE)

×: Disintegration point

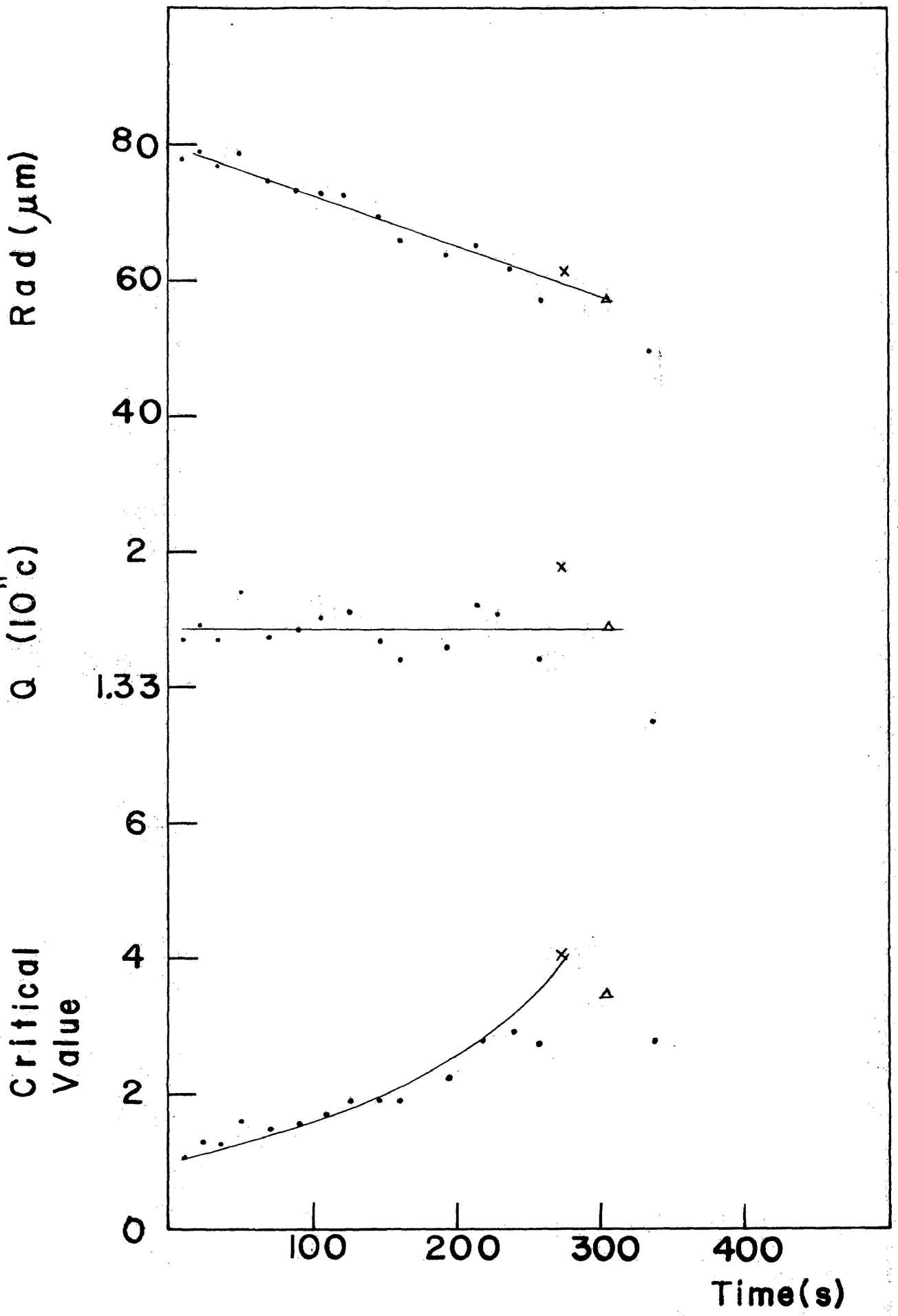

Fig.6-2 Radius, charge and critical value plotted against time for a typical positively charged drop

× : First disintegration point △ : Second disintegration point

TABLE 6-1: Data for figure 6-1

Time (s)	Radius (μ m)	Charge (10^{-11} C)	Critical Value
34	67.58	0.956	0.728
50	64.65	0.887	0.716
70	68.52	1.121	0.961
83	64.89	1.001	0.901
98	65.81	1.098	1.040
113	60.56	0.908	0.912
126	61.09	0.988	1.052
143	59.40	0.966	1.095
162	58.02	0.986	1.226
191	53.71	0.890	1.258
210	53.48	0.980	1.547
231	53.94	1.128	1.994
245	50.63	1.013	1.948
259	45.24	0.801	1.706

(NEGATIVE)

TABLE 6-2: Data for figure 6-2

Time(s)	Radius(μ m)	Charge (10^{-11}C)	Critical Value
10	78.79	1.541	1.194
22	79.53	1.653	1.335
36	76.68	1.536	1.287
50	79.38	1.805	1.602
70	74.50	1.570	1.467
90	73.41	1.602	1.595
107	73.53	1.690	1.767
126	72.37	1.710	1.897
145	68.33	1.556	1.867
160	65.81	1.460	1.838
191	63.71	1.526	2.215
217	64.81	1.758	2.793
239	61.72	1.672	2.925
257	56.82	1.423	2.712
274	61.37	1.943	4.019
302	56.94	1.631	3.543
336	48.97	1.153	2.785

(POSITIVE)

no measurable loss in the radius and charge at the first disintegration. The reason is probably that the mass and charge loss are small. From the critical function figures we know that after this disintegration the value of the critical function is lower, and the drop tends to stabilize. The second disintegration occurs with a 14% loss in radius, that is 36.4% loss in mass, and 28.9% loss in charge. Again, the value of the critical function tends to an even lower value. Figures 6-2a, 6-2b and 6-2c show the graphs on a larger scale.

The average radius loss in the measurement is 8.041% and the average charge loss is 20.788%: that is quite close to the prediction of Abbas and Latham. Table 6-3 shows the values of charge and radius loss for 9 cases.

The absolute value of the critical function is always higher than expected. (Rayleigh's criterion predicts 1. The average value in this experiment is 3.78.) However, the experimental result still shows a very good prediction; the disintegration happens when the value of critical function reaches a highest point and regains stability after disintegration.

Figure 6-3a shows the radius vs charge at the disintegration point. The result is not close to the theoretical prediction. The theoretical result predicts $k_1Q^2/16\pi R^3\gamma = 1$, while the average experimental result is close to $k_1Q^2/16\pi R^3\gamma = 3.78$. The values of radius and especially charge are unreasonably high at the disintegration point. This will be discussed later. If we believe that there is no possibility for the charge on the drop to increase during the measurement, we can take the average value of charge measured before the disintegration to correct the higher value. Figure 6-3b shows a graph of radius vs

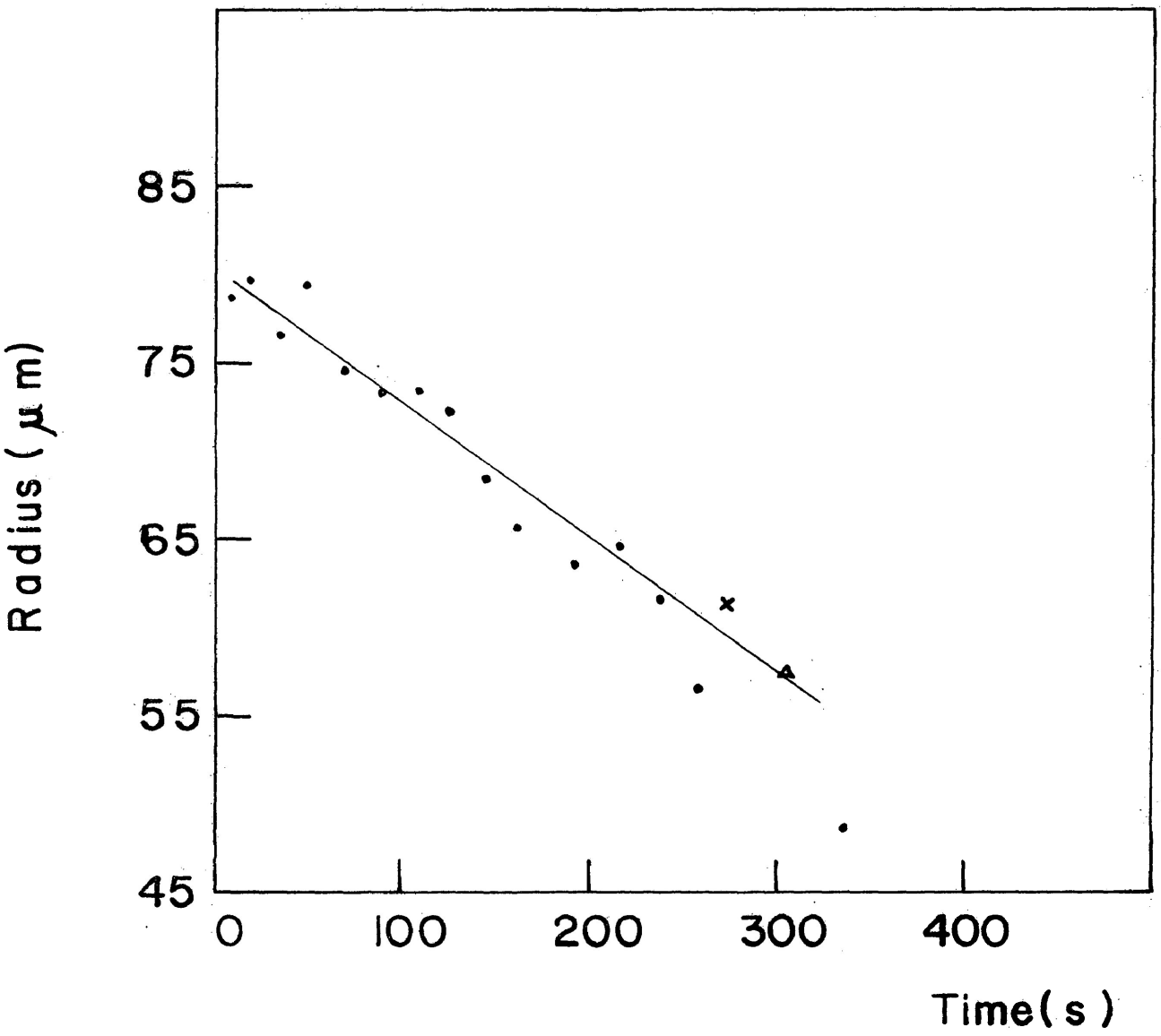

Fig. 6-2a Graph of radius vs. time (POSITIVE)

×: First disintegration point

△: Second disintegration point

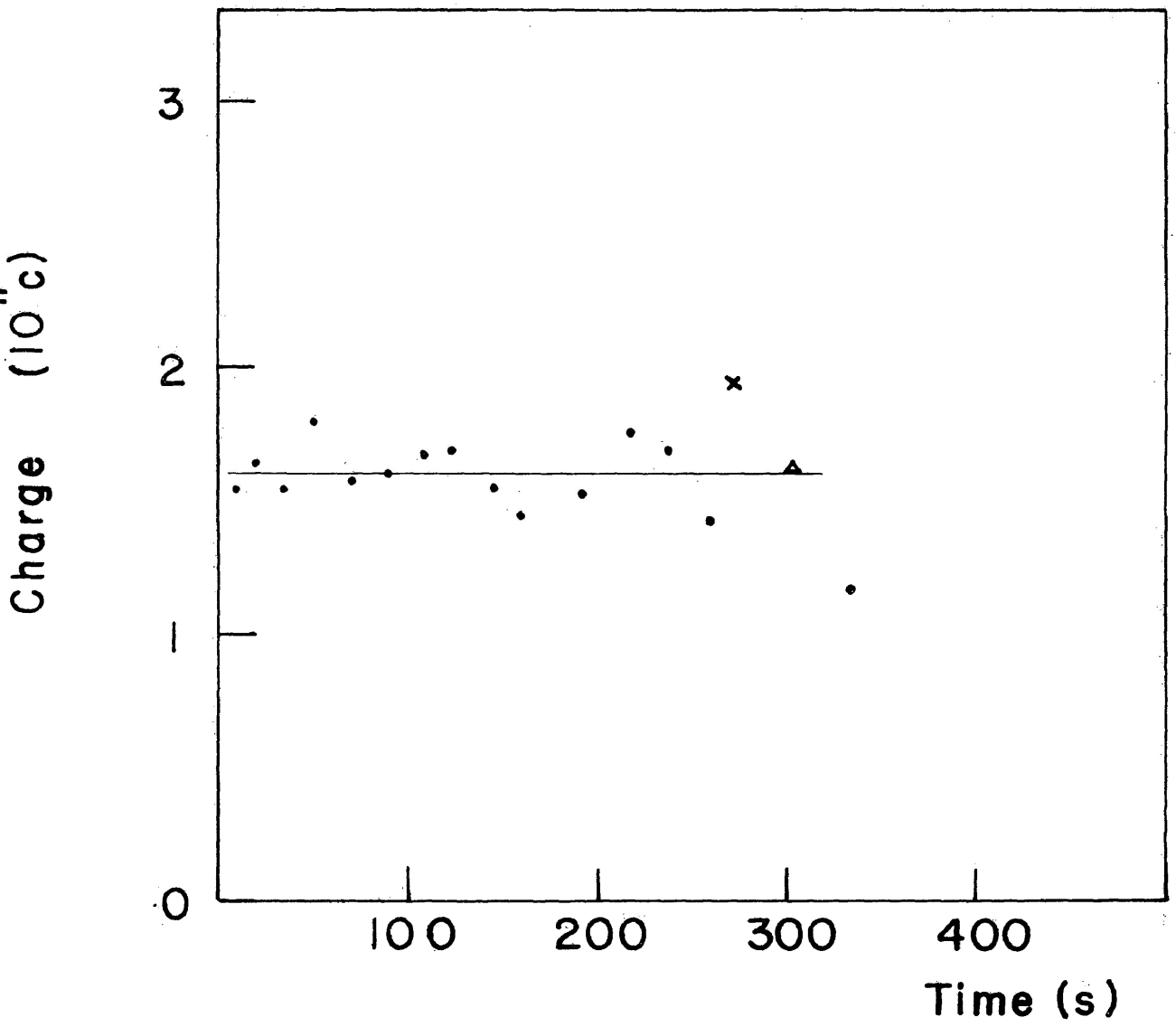

Fig. 6-2b Graph of charge vs. time (POSITIVE)

✕ : First disintegration point

▲ : Second disintegration point

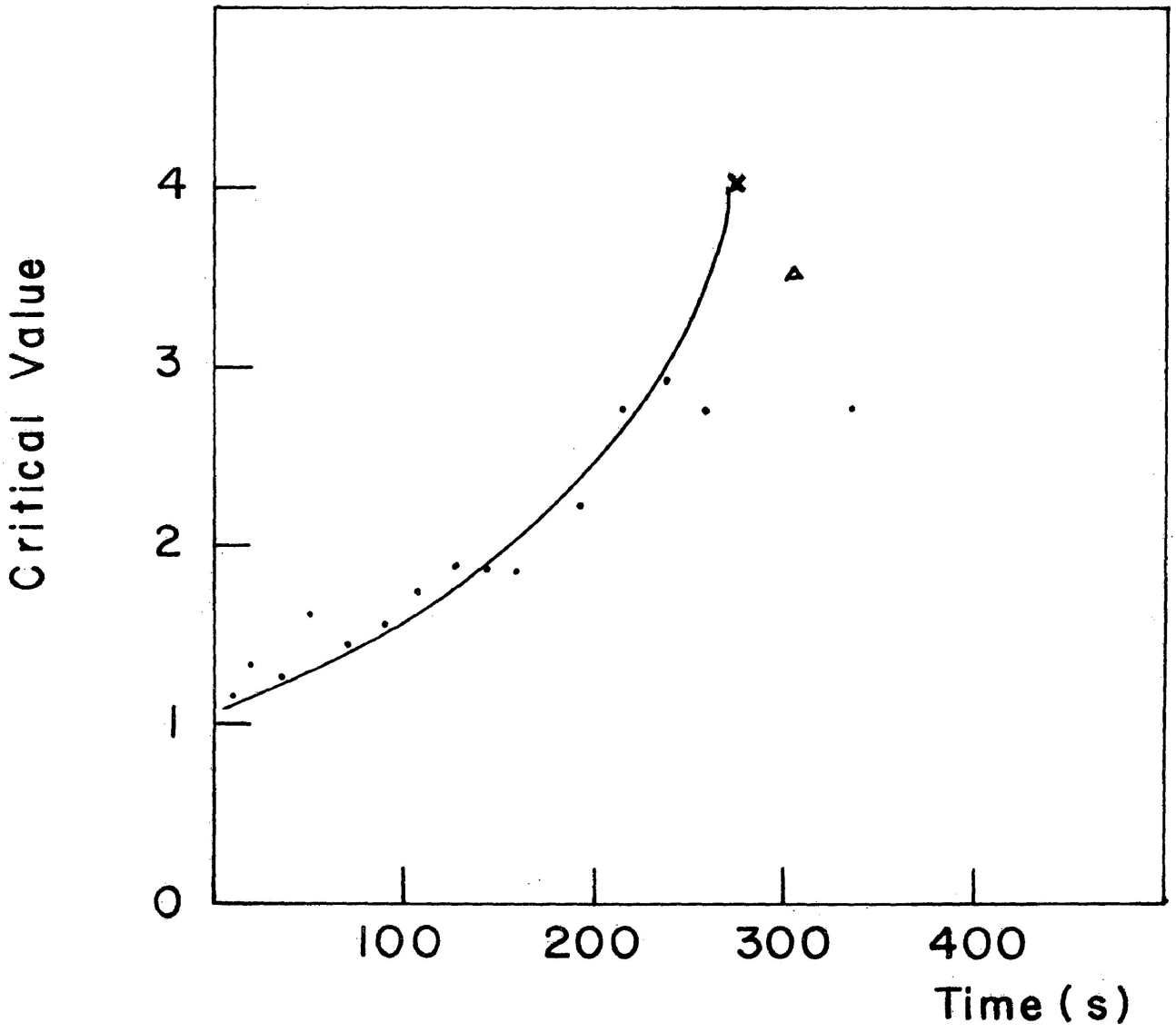

Fig. 6-2c Graph of critical value vs. time (POSITIVE)

X : First disintegration point

Δ : Second disintegration point

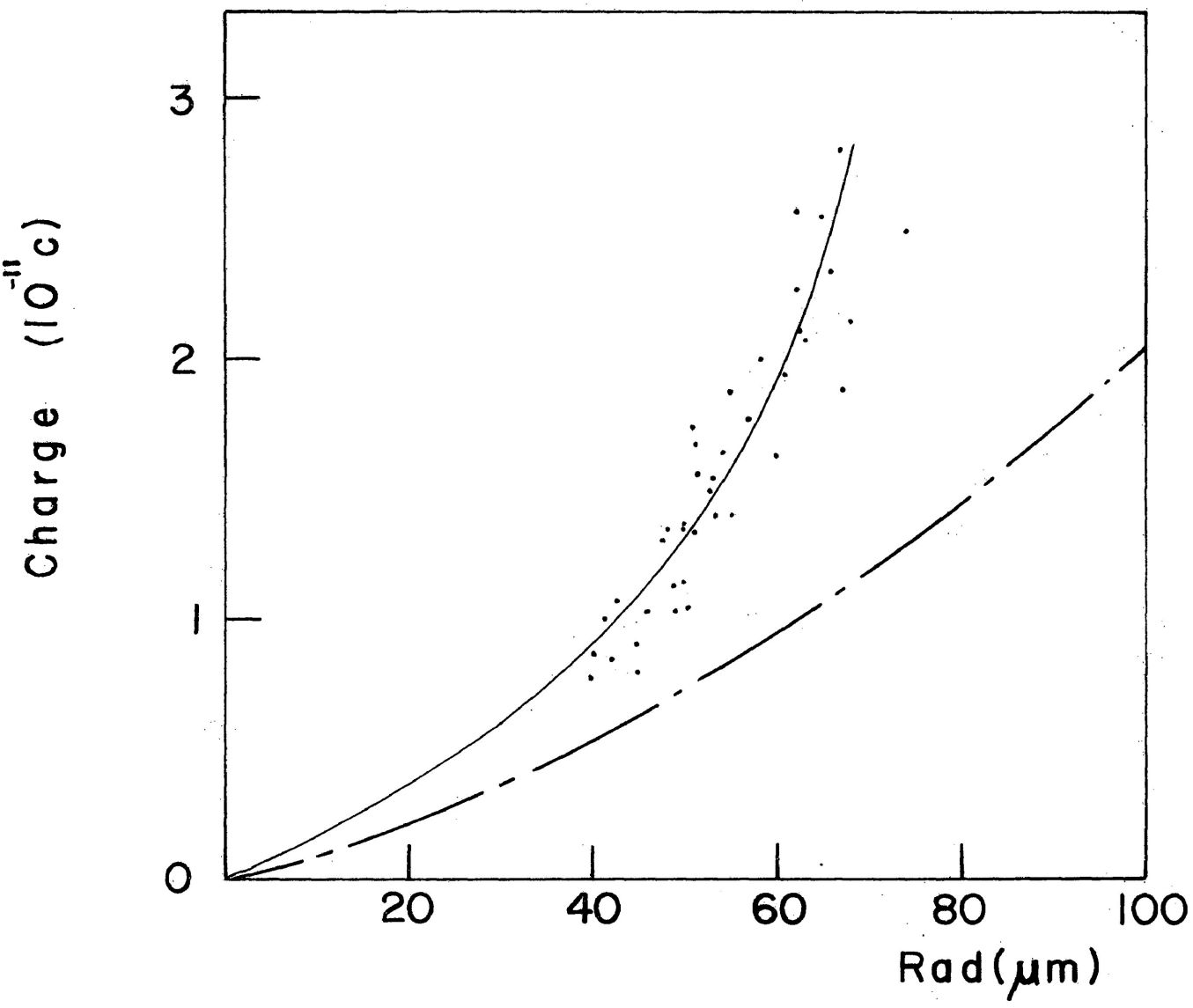

Fig. 6-3a The radius vs. charge at disintegration point

——- —— predicted by Rayleigh's Criterion

———— our experimental results

(BOTH SIGNS)

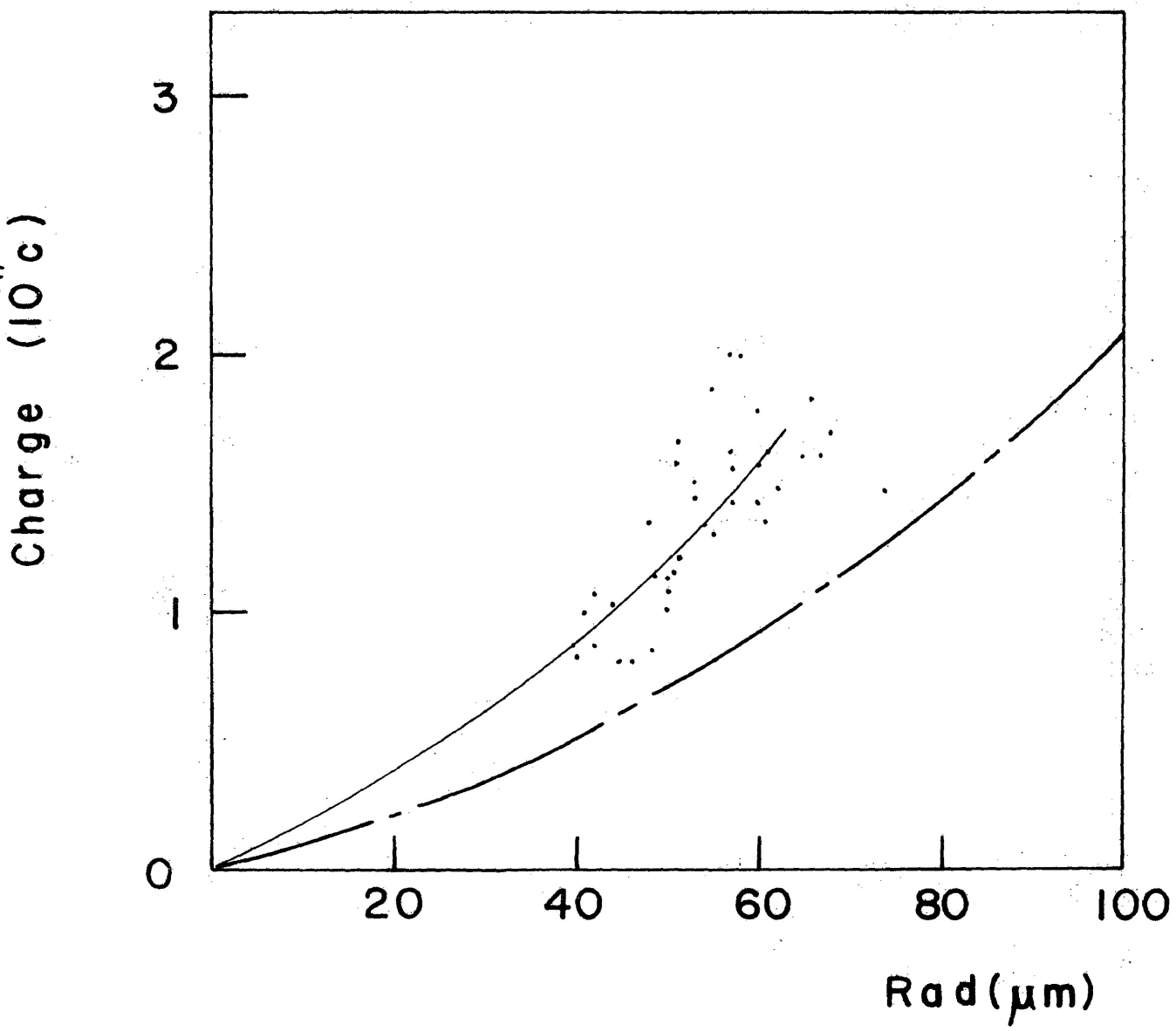

Fig. 6-3b The radius vs. charge at disintegration point

(after correction)

——·—— predicted by Rayleigh's Criterion

———— our experimental results

(BOTH SIGNS)

TABLE 6-3: Data for 9 cases of Radius and Charge Loss

Case	Radius loss (%)	Equivalent mass loss(%)	Charge loss(%)
1	8.91	24.42	19.92
2	9.64	26.22	21.64
3	6.22	17.53	19.4
4	14	36.40	28.98
5	7.71	21.40	7
6	6.14	17.32	13.23
7	8.04	22.24	30.10
8	9.08	24.84	27.79
9	6.275	17.67	19.03

(BOTH SIGNS)

corrected charge. The critical value given by this corrected charge is 2.422 which is still somewhat larger than the theoretical value of 1. Exact data are shown in Table 6-4. One possible fault in the measurement is the non-uniformity of the electric field. The field as made slightly non-uniform in order to keep the drop in the central region of the electrodes. For a non-uniformity of around 1% the effect on the result of measurement could be around 6%.

Other workers have not presented enough detailed data in their papers to allow me to check their results. It is hard to believe that the difference between their results and mine is due to a large systematic error in my experiment. The possibility of a 'supercritical' condition probably needs to be re-considered. Bacause of the symmetry of the drop, when the critical point is reached, the drop probably could pass the critical point and a 'supercritical' condition probably exists. The other possibility comes from Rayleigh's criterion, $k_1Q^2/4\pi(n + 2)R^3\gamma$, when n is an integer larger or equal to 2. Earlier workers all agree that the critical value is reached when n is equal to 2. However, according to the formula, the critical value could go higher when n is larger than 2. It is possible that values of n that are larger than 2 have a physical meaning, and that the drop be stable when the critical function is much larger than 1.

The drop always falls faster just before the disintegration point. This causes the higher values of the calculated radius and charge. (See figure 6-2.) For the first disintegration point, the radius is 61.37 μm, while it should be 59 μm by prediction. The charge is 1.943×10^{-11} C, while it should be 1.63×10^{-11} C. If we believe that the mass of the drop cannot increase, the only explanation is that the charge leaks. Because of

TABLE 6-4: Data for figure 6-3a, b

Radius(μm)	Charge (10^{-11}C)	Crit.	Est. Charge (10^{-11}C)	Est. Crit.
62	2.56	6.877	1.467	2.22
67.44	1.895	2.878	1.609	2.076
68.04	2.161	3.646	1.697	2.24
73.89	2.509	3.837	1.823	2.842
65.56	2.561	5.727	1.614	2.273
60.10	1.631	3.010	1.454	2.394
55.54	1.874	5.039	1.874	5.039
51.70	1.352	3.250	1.201	2.567
67.30	2.806	6.349	1.433	2.726
51.06	1.692	5.294	1.692	5.294
62.95	2.115	4.409	1.770	3.566
63.55	2.086	3.3245	1.347	1.967
74.13	4.027	9.79	1.470	1.3048
42.27	0.866	2.441	0.866	2.441
40.71	0.883	2.842	0.883	2.842
50.28	1.39	3.7386	1.149	2.556
49.466	1.048	2.23	1.048	2.23
50.625	1.136	2.447	1.095	2.27
79.68	2.717	3.5886	2.119	2.28
44.1475	0.904	2.335	1.036	2.335

Radius(μm)	Charge (10^{-11}C)	Crit.	Est. Charge (10^{-11}C)	Est. Crit.
41.63	1.011	3.467	1.011	3.467
53.30	1.540	3.872	1.432	3.33
65.96	2.354	4.7439	1.560	2.878
57.22	1.781	4.1674	1.560	3.318
53.30	1.503	3.67	1.503	3.67
55.76	1.327	2.50	1.327	2.50
53.62	1.4	3.127	1.338	2.855
49.18	1.16	2.785	1.16	2.785
42.45	1.079	3.743	1.079	3.743
61.37	1.943	4.0186	1.622	2.799
56.94	1.631	3.542	1.631	3.542
47.787	1.314	3.891	0.842	1.596
50.625	1.014	1.9477	0.994	1.874
45.24	0.801	1.706	0.801	1.706
40.32	0.48	0.865	0.48	0.865
62.00	2.267	5.303	2.267	5.303
58.19	2.014	5.061	2.014	5.061
56.99	2.029	5.471	2.029	5.471
51.499	1.569	4.435	1.569	4.435
48.08	1.422	4.471	1.422	4.471
46.65	1.008	2.462	0.804	1.565
51.175	1.795	5.676	1.795	5.676
40.126	0.790	2.379	0.790	2.379

the high humidity inside the jar, the electrical conductivity of the humid air is probably very high too, but the exact figure is beyond the range of this thesis. The shape of the drop could also affect the result, but more theoretical calculations must be made before anything definite could be said.

6-2 The Uncertainty in the Experiment

The radius is calculated from:

$$R = \left(\frac{9\eta}{2\rho g}\right)^{\frac{1}{2}}\left(\frac{T}{(1 - \alpha)D}\right)^{\frac{1}{2}} . \qquad (6\text{-}2)$$

Suppose the viscosity η, density ρ and gravitational acceleration g are exact. The uncertainty comes from the time of falling T, the distance of falling D, and the ratio of reduced field to the balanced field α. The uncertainty of α was tested and found around $\pm$ 0.1%. The estimated uncertainties of T and D are around 10% each. Thus, there is a total of 10% uncertainty in the radius measurement.

The charge is calculated from:

$$Q = \frac{4\pi\rho g\alpha d R^3}{3\ V_r} , \qquad (6\text{-}3)$$

where d is the distance between two electrodes. Its uncertainty is estimated as $\pm$ 1.5%. V_r is the reduced voltage recorded during the measurement. Its estimated uncertainty is around 5%. The total uncertainty in the charge measurement is thus 36.6%.

The critical function can be expressed as:

$$\text{crit.} = \frac{3\pi\rho^{\frac{1}{2}} g^{\frac{1}{2}} \eta^{\frac{3}{2}}}{2\sqrt{2\gamma}} \left[\frac{d^2\alpha^2}{V_r^2 (1 - \alpha)^{\frac{3}{2}}}\right]\left(\frac{D}{T}\right)^{\frac{3}{2}} . \qquad (6\text{-}4)$$

According to the uncertainties estimated above, the total uncertainty of the critical function is around $\pm$ 49.2% !

The uncertainties of charge and critical function are quite large. This is caused by the uncertainty of measuring time T and the distance D. Usually, the falling time of a 90 μm radius drop is around 2.5 s. It is very hard to judge the drops exactly by using the human eye. There are two ways to solve this problem. One is to set up a photocell to detect the drops automatically when they pass the line. The other way is to use a sensitive TV camera to take a slow motion picture and then replay it to determine the time and distance. But, both of these have some disadvantages. In either case, the equipment has to be sensitive to avoid the heating problem.

The uncertainty of the ratio of the reduced field to the balanced field is a very 'dangerous' factor. If we have a ratio $\alpha = 0.975 \pm 0.3\%$, the uncertainty in the critical function will be 18.6%. The ratio has been tested by a precision voltmeter and the uncertainty is around 0.1% in this measurement.

6-3 The External Electric Field Affects the Results

In 1970, G. A. Dawson mentioned in his paper, *The Rayleigh Instability of Water Drops in the Presence of External Electric Fields*, that the shape of the drop will be distorted near the instability point by the external electric field. The radial electric field of the drop is four orders of magnitude larger than the levitating field in the beginning of the experiment. For a drop of radius 100 μm and charge 1.67×10^{-11} C, the radial electric field is 1.57×10^{7} V/m, while the levitating field is 2.46×10^{3} V/m. As Rayleigh's criterion is approached, the excess pressure inside the drop, which causes the spherical shape, decreases to zero, so the small levitating field will be able to produce appreciable distortion of the drop. This distortion

would not cause too much effect (about 2.5%) on the final charge when instability occurs for drops of radius below 250 μm. Thus, the experiment probably is not perfectly suited for checking Rayleigh's criterion, but is still a very useful one, especially since the electric field in the atmosphere is around the same value as is used in the laboratory.

In 1972, P. R. Brazier-Smith mentioned in his paper, *The Stability of Charged Drops in a Uniform Electric Field*, that the spheroidal assumption is not suitable for charged droplets. He pointed out that, if we consider the pressures on the upper pole, lower pole and equator, the shape of the drop and stability criterion are quite different from what Dawson found. He calculates the shape of the drop in the external electric field. This criticism is again theoretical and the difference probably could not be detected in the laboratory. Thus, there seems to be no better way to verify Rayleigh's criterion than the way it has been done by Doyle et al, Abbas and Latham, and Dawson.

6-4 The Evaporation Affects the Measurment

The equations that are used to determine the radius R and the charge Q were derived under the assumption that the volume of the drop does not change during the measurement. The fact that the drop is evaporating while it falls does introduce some error. An estimate of this error will be made here.

If we assume that the ambient conditions (temperature, pressure, and humidity) do not change during measurement, the specific surface evaporation rate J can be defined as the volume loss per unit area A per unit time. That is:

$$J = \frac{dV}{Adt} . \qquad (6\text{-}5)$$

If we assume the drop is spherical and the density is uniform, then:

$$dV = 4\pi R^2 dR \ . \tag{6-6}$$

Since the surface area of the drop is $A = 4\pi R^2$, the specific surface evaporation rate is just:

$$J = \frac{dR}{dt} \ . \tag{6-7}$$

The rate of volume loss is

$$\frac{dV}{dt} = 4\pi R^2 \frac{dR}{dt} \ . \tag{6-8}$$

Substituting (6-7) into (6-8), we get

$$\frac{dV}{dt} = 4\pi R^2 J \ . \tag{6-9}$$

Then the percentage volume loss in the time dt is

$$\frac{dV}{V} \times 100\% = \frac{3Jdt}{R} \times 100\%. \tag{6-10}$$

From this equation we see that, when the specific surface evaporation rate is large or the radius of the drop is small, the percentage of volume loss in a time interval dt is large. Now, consider the equations we use for measurement:

$$\frac{4}{3} \pi R^3 \rho g = QE_b \tag{6-11}$$

$$\frac{4}{3} \pi R^3 \rho g - Q E_r = 6\pi \eta RV \ . \tag{6-12}$$

The reduced field is about 2.5% less than the balanced field in the experiment. If the volume is decreasing rapidly, the left side of equation (6-12) will change to zero or negative in a short period of time, that is, the velocity of falling changes to zero or negative.

This is the reason that the drop will stop falling and then rise up in some cases.

If the radius of the drop is small, then according to the equation (6-10), the percentage volume loss is large. Suppose J = 0.078 μm/sec, t = 25 s, R = 25 μm; the percentage volume loss will be 25%. It turns out that the balanced field is hard to stabilize, and it is necessary to reduce the field continuously to balance the drop. In this case the measurement becomes impossible. Thus, a low evaporation rate is necessary if we wish to measure the radius and the charge of small drops.

If the temperature of the system is increasing during the measurement, then the evaporation rate will also be increasing and this will affect the measurement.

The following sample calculation shows how the radius of a drop affects the percentage volume loss.

If J = 0.078 μm/s , dt = 2.7 s , and R = 78.79 μm, then

$$\frac{dV}{V} \times 100\% = \frac{3 \times 0.078 \times 2.7}{78.79} \times 100\% = 0.802\% \quad .$$

On the same evaporation rate, when the radius is becoming smaller, the percentage volume loss is increasing. When the radius is smaller, but the evaporation rate is the same:

J = 0.078 μm/s , dt = 6.99 s , R = 48.96 μm

then

$$\frac{dV}{V} \times 100\% = \frac{3 \times 0.078 \times 6.99}{48.96} \times 100\% = 3.34\% \quad .$$

From the example, the effect of the evaporation rate is easy to see. If the evaporation rate is just one-tenth of the above number, even in the small radius case (25 μm) the volume loss is still small (2.5%) and the measurement is possible.

7. CONCLUSION

The results of the experiment are quite reproducible. Although the value of critical function is higher than it should be, it still predicts the disintegration quite well. The mass loss after the disintegration is around 23%, and the charge loss is around 20%. This result is quite close to the result of Abbas and Latham. Dawson mentioned in his paper that the mass loss is just few percent after disintegration; actually it is hard to tell the difference of a few percent with the method of measurement used in this kind of experiment. The difference in mass loss probably is not related to the evaporation rate directly. The changing ambient condition (fluctuation of temperature, low humidity) seems more likely.

In my experiment high humidity is reached before the measurement, and the measurement is performed at the most stable temperature. Thus, the effect of the ambient situation is reduced to the minimum. However, in order to know the exact effect, a further experiment will be necessary, probably involving a controllable temperature system, precision hygrometer, an improved method for measurement, reducing the heat transfer from the light source and a more uniform field.

A low pressure experiment could be very interesting too, because it is closer to the situation in the atmosphere. That was the basic reason for using the enclosed vacuum system as a design norm. Although the external field used in this experiment will affect the shape of the drop when it approaches the disintegration point, the field is close to the field to be found in the vicinity of electrified clouds and the surface of lakes and oceans (500 - 2000 V/m). So, if there are no other complicating factors,

such as corona discharge (Dawson, 1969),an evaporating droplet in the atmosphere would behave much the same way as in the laboratory.

APPENDIX I Some Details of the Calculation of Rayleigh's Criterion

I-1 The Calculation of the Volume

$$V = \frac{2}{3}\pi\int_{-1}^{1} a_0^3\left[1 + 3\sum_n \frac{a_n}{a_o} P_n(\mu) + 3\sum\sum_{nm} \frac{a_n a_m}{a_0^2} P_n(\mu)\, P_m(\mu)\right]d\mu$$

The three terms of integration I_1, I_2, I_3 are:

$$I_1 = \frac{2}{3}\pi\int_{-1}^{1} a_0^3 du = \frac{4}{3}\pi a_0^3 \qquad \text{(I-1)}$$

$$I_2 = \frac{2}{3}\pi\int_{-1}^{1} 3a_0^2 \sum_n a_n P_n(\mu)d\mu$$

$$= 2\pi a_0^2 \int_{-1}^{1} \sum_n a_n P_n(\mu)d\mu$$

$$= 2\pi a_0^2 \sum_n a_n \int_{-1}^{1} P_n(\mu)\, P_o(\mu)d\mu \qquad \because P_0(\mu) = 1$$

$$= 2\pi\, a_0^2 \sum_n a_n \frac{2}{2n+1} \delta_{no} \qquad \text{(This is orthogonal condition for the Legendre Equation.)}$$

$$= 0 \qquad \text{(Because n is an integer equal to 1 .....}\infty\text{, but not zero.)} \qquad \text{(I-2)}$$

$$I_3 = \frac{2}{3}\pi\int_{-1}^{1} 3a_0 \sum_n \sum_m a_n a_m P_n(\mu) P_m(\mu)d\mu$$

$$= 2\pi a_0 \sum\sum_{nm} a_n a_m \int_{-1}^{1} P_n(\mu)\, P_m(\mu)d\mu$$

$$= 2\pi a_0 \sum_{nm}\sum a_n a_m \frac{2}{2n+1} \delta_{n,m}$$

$$= 2\pi a_0^3 \sum_n \frac{2}{2n+1} \frac{a_n^2}{a_0^2} \qquad \text{(I-3)}$$

Combining (I-1), (I-2) and (I-3), we get

$$V = \frac{4}{3}\pi a_0^3 + 0 + 2\pi a_0^3 \sum_n \frac{2}{2n+1} \frac{a_n^2}{a_0^2}$$

$$= \frac{4}{3}\pi a_0^3 \left(1 + \sum_n \frac{3}{2n+1} \left(\frac{a_n}{a_0}\right)^2\right)$$

$= \frac{4}{3}\pi a^3$ Because $\frac{a_n}{a_0} << 1$, use the reverse of binomial theorem.

Here, we let $a = a_0\left(1 + \sum_n \frac{1}{2n+1} \left(\frac{a_n}{a_0}\right)^2\right)$.

I-2 Calculation of the Surface Area

$$S = \int_0^{2\pi}\int_{-1}^{1} r^2 d\mu d\phi + \frac{1}{2}\int_0^{2\pi}\int_{-1}^{1} \sum_{mn}\sum a_n a_m \frac{dP_n(\mu)}{d\mu}\frac{dP_m(\mu)}{d\mu}(1-\mu^2)d\mu d\phi.$$

The first integral on the right is:

$$S_1 = \int_0^{2\pi}\int_{-1}^{1} r^2 d\mu d\phi$$

$$= 2\pi \int_{-1}^{1} r^2 d\mu$$

$$= 2\pi \int_{-1}^{1} (a_o + \sum_{n=1} a_n P_n(\mu))^2 \, d\mu$$

$$= 2\pi (2a_0^2 + 2\sum_{n=1} (2n + 1)^{-1} a_n^2).$$

In the second term, we use the formula

$$\int_{-1}^{1} (1 - \mu^2) \frac{dP_n(\mu)}{d\mu} \frac{dP_m(\mu)}{d\mu} d\mu = n(n + 1) \int_{-1}^{1} P_n(\mu) P_m(\mu) d\mu$$

which is valid whether n is equal to, or different from, m.

The second term S_2 is:

$$S_2 = \frac{1}{2} 2\pi \sum_{m,n} a_n a_m \, n(n + 1)(2n + 1)^{-1} \, 2\delta_{n,m}$$

$$= 2\pi \sum_{n} n(n + 1)(2n + 1)^{-1} a_n^2 .$$

Therefore, the total area is:

$$S = 4\pi a_o^2 + 4\pi \sum_{n=1} (2n + 1)^{-1} a_n^2 + 2\pi \sum_{n=1} n(n + 1)(2n + 1)^{-1} a_n^2$$

I-3 Calculation of Charge Density and Potential

$$4\pi\sigma = - \frac{\partial \Phi}{\partial r} \Big| \; r = a + \sum_{n} a_n P_n(\mu)$$

$$= k_1 Q r^{-2} + k_1 \sum_{n=1} (n + 1) Q r^{-n-2} \, a^{n-1} \, P_n(\mu) \, a_n$$

$$= k_1 Q \, (a + \sum_{n} a_n P_n)^{-2} + k_1 \sum_{n=1} (n + 1) Q (a + \sum_{n} a_n P_n)^{-n-2} a^{n-1} P_n(\mu) a_n$$

$$= k_1 Q a^{-2}\left(1 - 2\sum_n \frac{a_n}{a} P_n\right) + k_1 \sum_{n=1} (n+1) Q a^{-n-2}\left(1 - \sum_n (n+2)\frac{a_n}{a} P_n\right) a^{n-1} P_n(\mu) a_n$$

$$= k_1 \frac{Q}{a^2} - k_1 2Q \sum_n \frac{a_n}{a^3} P_n + k_1 \sum_{n=1} (n+1) Q a^{-n-2} a^{n-1} P_n(\mu) a_n$$

$$= k_1 \frac{Q}{a^2} - k_1 2Q \sum_n \frac{a_n}{a^3} P_n(\mu) + k_1 \sum_{n=1} (n+1) \frac{Q}{a^3} P_n(\mu) a_n$$

$$= k_1 \frac{Q}{a^2} + k_1 Q \sum_n \frac{(n-1) a_n}{a^3} P_n(\mu)$$

In the above calculation terms of order a_n^2 were neglected because they are small.

The electrostatic potential of the drop, Φ, is calculated by using

$$\Phi = \int \frac{\sigma}{r} dA \quad .$$

$$\Phi = \int_0^{2\pi} \int_{-1}^{1} \frac{\sigma r^2}{r} d\mu d\phi$$

$$= 2\pi \int_{-1}^{1} \sigma r d\mu$$

$$= 2\pi \int_{-1}^{1} \frac{k_1 Q}{4\pi a^2} \left[1 + \sum_n (n-1) \frac{a_n P_n}{a}\right]\left[1 - \sum_n \frac{a_n P_n}{a}\right] a d\mu$$

$$= \frac{1}{2}\int_{-1}^{1} \frac{k\,Q}{a}\left[\,1 + \sum_n (n-1)\,\frac{a_n P_n}{a}\right]\left[\,1 - \sum_n \frac{a_n P_n}{a}\,\right] d\mu$$

$$= \frac{1}{2}\int_{-1}^{1} \frac{k_1 Q}{a}\left[\,1 - \sum_n \frac{a_n P_n}{a} + \sum_n (n-1)\frac{a_n P_n}{a} - \sum_n (n-1)\frac{a_n^2 P_n^2}{a^2}\,\right] d\mu \quad .$$

The first term is

$$\Phi_1 = \frac{k_1 Q}{a} \quad .$$

The second and third terms are zero because of the single $P_n(\mu)$ terms and n starts from 1 by definition. (Also see Appendix I-1.)

By direction integration, the fourth term is:

$$\Phi_4 = -\frac{k_1 Q}{a} \sum_n \frac{n-1}{2n+1}\frac{a_n^2}{a^2} \quad .$$

Combining the results above, we get:

$$\Phi = \frac{k_1 Q}{a} - \frac{k_1 Q}{a} \sum_n \frac{n-1}{2n+1}\frac{a_n^2}{a^2} \quad .$$

APPENDIX II An A.P.L. program for calculating the radius, charge and critical value of the drops.

```
     ∇ MESU
[1]    T1←0,T
[2]    T2←T,A
[3]    T3←T2-T1
[4]    E←V÷(0.975×0.113)
[5]    R←0.0001×((9×1.827×5)÷(2×9.81×2.5×T3))*0.5
[6]    Q←(10×4×01×981×R*3)÷(3×E)
[7]    CRIT←(9×1000000000×Q*2)÷(16×72.8×0.001×01×R*3)
[8]    'THE TIME OF FALLING ARE'
[9]    T3
[10]   'THE LEVITATED ELECTRIC FIELD ARE '
[11]   E
[12]   'THE RADIUS OF THE DROP ARE '
[13]   R
[14]   'THE CHARGE OF THE DROP ARE '
[15]   Q
[16]   'THE RALEIGHS CRITERION ARE'
[17]   CRIT
     ∇
```

APPENDIX III Sample Calculations of Charge, Radius and Critical Value

The equations used for measurements are:

$$R^2 = \frac{9\eta}{2\rho_\omega g}\left(\frac{D}{(1 - \frac{Er}{E_b})T}\right) \tag{2-44}$$

$$Q = \frac{4}{3}\pi R^3 \rho_\omega g E_b^{-1} \tag{2-38}$$

The constants used in the calculations are:

viscosity $\eta = 1.827 \times 10^{-5}$ kg/msec

density $\rho_\omega = 10^3$ kg/m^3

acceleration of gravity g = 9.81 m/sec^2

ratio of reduced field to balanced field $\frac{E_r}{E_b} = 0.975$

distance of fall D = 0.05 m

distance between the two electrodes d = 0.113 m.

The time of falling and reduced voltage measured at the disintegration point of figure 6-1 are 6.54 s and 57.95 V.

So, the balanced electric field is

$$E_b = 57.95 \div 0.975 \div 0.113 = 526 \text{ V/m}.$$

The radius R is equal to:

$$R = \left(\frac{9 \times 1.827 \times 10^{-5}}{2 \times 10^3 \times 9.81} \times \frac{0.05}{0.025 \times 6.54}\right)^{\frac{1}{2}}$$

$$= 50.62 \text{ } \mu\text{m}.$$

Substituting R and E_b into (2-45), we get

$$Q = \frac{4}{3}\pi\ (50.62 \times 10^{-6})^3 \times (10^3) \times (9.81) \div (526)$$

$$= 1.013 \times 10^{-11}\ \text{C}.$$

The critical value can be expressed as:

$$\frac{k_1 Q^2}{4\pi(n + 2)R^3\gamma}$$

where surface tension $\gamma = 72.8 \times 10^{-3}$ N/m,

$k = 9 \times 10^9 \frac{Nm^2}{c^2}$,

and integer $n = 2$.

We find the critical value to be 1.95.

REFERENCES

1. Abbas, M. A., & Latham, J. *The Instability of Evaporating Charged Drops*. Fluid Mech. 30:4, 663-670, 1967.

2. Brazier-Smith, P. A. *The Stability of Charged Drops in Uniform Electric Fields*. Quart. J. R. Met. Soc. 98, 434-439, 1972.

3. Dawson, G. A. *The Pressure of Waterdrop Corona Onset and Its Atmospheric Importance*. J. Geophysics Res. 74:28, 6859-6868, 1969.

4. Dawson, G. A. *The Rayleigh Instability of Waterdrops in the Presence of External Field*. J. of Geophys. Res. 75:3, 701-705, 1970.

5. Dawson, G. A. *Charge Loss Mechanism of Highly Charged Water Droplets in the Atmosphere*. J. of Geophys. Res. 78:27, 6364-6369, 1973.

6. Dimmock, N. A. *Production of Uniform Droplets*. Nature, (London) 166, 686, 1950.

7. Doyle, A., Moffet, D. R. and Vonnegut, B. *Behaviour of Evaporating Electrically Charged Droplets*. J. of Colloid. Sci. 19, 136-143, 1964.

8. Mason, B. J., Jayaratne, O. W. and Woods, J. D. *An Improved Vibrating Capillary Device for Producing Uniform Water Droplets of 15 to 500 μm Radius*. J. Sci. Instrum. 40, 247-249, 1963.

9. Millikan, R. A. Electrons (+ and -), Protons, Photons, Neutrons and Cosmic Rays. Cambridge University Press, 1935.

10. Rayleigh, L. *On the Capillary Phenomena of Jets*. Proc. Roy. Soc. A29, 71-97, 1879.

11. Rayleigh, L. *On the Equilibrium of Liquid Conducting Masses Charged with Electricty*. Phil. Mag. 14, 184-186, 1882.

12. Schotland, R. M. *Experimental Results Relating to the Coalescence of Water Drops with Water Surface*. Disc. Faraday Soc. 30, 72, 1960.

13. Taylor, G. *Disintegration of Water Drops in an Electric Field*. Proc. Roy. Soc. (London) A280, 383-397, 1964.